Clim. Past Discuss., doi:10.5194/cp-2017-21, 2017
Manuscript under review for journal Clim. Past
Discussion started: 24 February 2017

Climate of the Past Discussions

Regional and global climate for the mid-Pliocene using CCSM4 and PlioMIP2 boundary conditions

Deepak Chandan[1] and W. Richard Peltier[1]

[1]Department of Physics, University of Toronto, 60 St. George Street, Toronto, Ontario, M5S1A7

Correspondence to: Deepak Chandan (dchandan@atmosp.physics.utoronto.ca)

Abstract. The Pliocene Model Intercomparison Project, Phase 2 (PlioMIP2) is an international collaboration to simulate the climate of the mid-Pliocene interglacial, marine isotope stage KM5c (3.205 Mya), using a wide selection of climate models with the objective of understanding the nature of the warming that is known to have occurred during the broader mid-Pliocene warm period. PlioMIP2 builds upon the successes of PlioMIP by shifting focus onto a specific interglacial and by using a revised set of geographic and orbital boundary conditions. In this paper, we present the details of the mid-Pliocene simulations that we have performed with the Community Climate System Model version 4 (CCSM4), and the 'enhanced' variant of the PlioMIP2 boundary conditions, and discuss the simulated climatology through comparisons to our control simulations, and to proxy reconstructions of the climate of the mid-Pliocene. With the new boundary conditions, the CCSM4 model simulates a mid-Pliocene which is more than twice as warm as that with the boundary conditions used for PlioMIP Phase 1. The warming is more enhanced near the high-latitudes which is where most of the changes to the boundary conditions have been made. The elevated warming in the high-latitudes leads to a better match of the simulated climatology to proxy based reconstructions than what was possible with the previous version of the boundary conditions.

1 Introduction

The mid-Pliocene warm period, 3.3-3 million years ago, was the most recent time period during which the global temperature was higher than present for an interval of time longer than any of the Pleistocene interglacials. The prevalence of widespread warming during this time has been inferred from proxy based sea surface temperature (SST) reconstructions from a number of widely distributed deep-sea sedimentary cores (*Robinson et al.*, 2008; *Lawrence et al.*, 2009; *Dowsett et al.*, 2010; *Fedorov et al.*, 2012). The PRISM (Pliocene Research, Interpretation and Synoptic Mapping) version 3 (PRISM3, *Dowsett et al.*, 2010) compilation of mid-Pliocene SSTs contains data from 100 sites. In contrast, surface air temperature (SAT) estimates are more difficult to reconstruct owing to limited availability of land based proxies that are useful for palaeo-thermometry. However, some records available from high-latitudes in the northern hemisphere provide an important perspective on the magnitude of warming in that region. *Rybczynski et al.* (2013) found mid-Pliocene plant fossils in peat deposits at Ellesmere Island (north of the Arctic circle in the Canadian archipelago) which led them to estimate that the local mean annual SAT during the mid-Pliocene was

Clim. Past Discuss., doi:10.5194/cp-2017-21, 2017
Manuscript under review for journal Clim. Past
Discussion started: 24 February 2017

Climate of the Past Discussions

$18.3 \pm 4.1°C$ warmer than present while summer temperature hovered around $14°C$. (*Brigham-Grette et al.*, 2013) studied lacustrine records from arctic lake El'gygytgyn in NE arctic Russia on the basis of which they inferred that the summer temperature there was $\sim 8°C$ warmer than today.

The warming during the mid-Pliocene is expected to have resulted in a much higher eustatic sea level (ESL) owing to the melting of large amounts of polar ice. One of the earliest estimates for the mid-Pliocene ESL comes from *Dowsett and Cronin* (1990), who derived a local estimate based upon measurements of present day elevation above sea level of mid-Pliocene dated marine deposits in the Orangeburg Scarp, near the South Carolina and North Carolina border. After correcting the observed elevation for the regional long-term uplift rate, they arrived at a $+35 \pm 18$ m estimate of the mid-Pliocene ESL (the plus sign denotes sea level higher than present). This value was used to perform the first global reconstruction of the mid-Pliocene climate – PRISM1 (*Dowsett et al.*, 1994).

Based on an analysis of palaeoclimatic data from high-latitude deep-sea sediments, *Kennett and Hodell* (1993, 1995) argued for a mid-Pliocene sea level no more than +25 m and "probably significantly less than this for most of this interval". Their analysis led to the revising down of the sea level estimate for PRISM2 (*Dowsett et al.*, 1999) to +25 m. Subsequent versions of PRISM reconstruction, namely PRISM3 (*Dowsett et al.*, 2010) and PRISM4 (*Dowsett et al.*, 2016) also include a +25 m mid-Pliocene ESL. A number of other estimates for the ESL all fall in the range of +10 m to +30 m (*Wardlaw and Quinn*, 1991; *Krantz*, 1991; *Dwyer and Chandler*, 2009; *Naish and Wilson*, 2009; *Rowley et al.*, 2013). *Miller et al.* (2012) performed a multi-proxy analysis using backstripped records from Virginia, New Zealand and the Enewetak Atoll, benthic foraminiferal $\delta^{18}O$ constraints and $Mg/Ca - \delta^{18}O$ estimates to argue that the mid-Pliocene sea level was, within a two standard deviation margin, 22 ± 10 m higher than present. More recently, *Winnick and Caves* (2015) have argued for a reexamination of the transfer function that is used to convert mid-Pliocene benthic $\delta^{18}O$ measurements to sea level in order to correct for the changing $\delta^{18}O$ content of Antarctic ice. On the basis of the revised transfer function, they estimate that the mid-Pliocene ESL was only 9-13.5 m higher than present.

Although estimates for the mid-Pliocene ESL show considerable spread, all of them strongly suggest substantial or total loss of the most vulnerable ice sheets - the Greenland Ice Sheet (GIS) and the West Antarctic Ice Sheet (WAIS). The GIS contains ~ 7 m of ESL equivalent ice (*Alley et al.*, 2005) and is known to have been greatly diminished under the influence of the mid-Pliocene warmth (*Lunt et al.*, 2008; *Contoux et al.*, 2015). The WAIS which presently contains $\sim$5 m of ESL equivalent ice (*Fretwell et al.*, 2012) is mostly grounded below sea level and is therefore dynamically unstable to a runaway collapse (*Weertman*, 1974). Together the collapse of these two ice-sheets could contribute up to 12 m to the mid-Pliocene ESL. The largest of the present day ice sheets - the East Antarctic Ice Sheet (EAIS) is considered to be relatively stable owing to its bedrock lying mostly above sea level. However, the EAIS does contain a number of large subglacial basins the largest being the Wilkes and Aurora basins which are grounded below sea level and are therefore susceptible to collapse similar to the WAIS. Consequently, mid-Pliocene ESL estimate above 12 m imply substantial amounts of additional melting in the most vulnerable sectors of EAIS.

Clim. Past Discuss., doi:10.5194/cp-2017-21, 2017
Manuscript under review for journal Clim. Past
Discussion started: 24 February 2017

Climate of the Past Discussions

It would not be particularly surprising if the higher warming and the accompanying melting of the polar ice took place in a world with much higher radiative forcing from the presence of atmospheric greenhouse gases in higher concentrations. Instead, proxy reconstructions for the mid-Pliocene atmosphere do not show any significant increase in greenhouse gas concentrations compared to the preset day. Various reconstructions for the atmospheric CO_2 concentration, such as those based on alkenone data (*Pagani et al.*, 2010; *Seki et al.*, 2010; *Badger et al.*, 2013; *Zhang et al.*, 2013a), $\delta^{13}C$ measurements in marine organic matter (*Raymo et al.*, 1996), $\delta^{11}B$ measurements (*Seki et al.*, 2010; *Bartoli et al.*, 2011; *Martínez-Botí et al.*, 2015), foraminiferal B/Ca ratio based estimates (*Tripati et al.*, 2009) and estimates from stomatal density in fossilized leaves (*Kürschner et al.*, 1996) show that during the mid-Pliocene CO_2 varied between ~ 200 ppmv and ~ 450 ppmv, with most measurements reporting in the range of 300-400 ppmv. A value of 400 ppmv is often used as a boundary condition in atmosphere only and coupled-climate models.

Very little is known about the concentration of the very potent greenhouse gas methane, although it is expected to be at least as high as modern, if not higher, mainly due to its release from the thawing Arctic permafrost and from the breakdown of methane clathrates - both of which are expected consequences of a warm Arctic. In the absence of proxy estimates for methane concentration in the mid-Pliocene atmosphere, the modern day concentration value is usually used (for instance in the context of the PlioMIP program) in climate models. The uncertainty in the methane concentration is partly compensated for in climate models by choosing a higher concentration of CO_2 .

The inference of warm temperatures and reduced land ice during a time period when the atmosphere was characterized by greenhouse gases concentrations not much different that present, and significantly less than projections for the future, is the primary reason that the mid-Pliocene has received considerable interest in recent decades. Since the future of our climate will be 'Pliocene-like' it is of vital importance that we understand the magnitude and distribution of the mid-Pliocene warming, the mechanisms for the warming and the consequences of the warming.

The Pliocene Model Intercomparison Project (PlioMIP) was organized with the aim of understanding the magnitude and mechanisms of the degree of warmth that proxies are indicating, by using a diverse selection of climate models. Phase 1 of the project (henceforth simply PlioMIP) was concerned with simulating the averaged climate of all warm interglacials in a 300,000 year 'time-slab' during the mid-Pliocene. Results from the eights models participating in PlioMIP found significant difference between the temperature reconstructions produced by the models, and between the models and data. While the models successfully simulated an overall warmer climate with some amplification of warming in high-latitudes, they fell well short of capturing the magnitude of warming at high-latitudes that is indicated by the proxy based inferences (*Dowsett et al.*, 2013).

The outcomes of PlioMIP have helped in developing the revised strategy that is being employed in the context of PlioMIP2. The focus is now on a single warm interglacial, namely marine isotope stage KM5c (3.205 Mya). This approach is expected to improve the resolution of reconstructed temperature data and thereby improve confidence in it. On the modeling side, a new set of boundary conditions - the PRISM4 boundary conditions (*Dowsett et al.*, 2016) are available for modeling groups to use. In this paper we will employ these new boundary conditions in an attempt to better understand what the characteristic of the climate of the mid-Pliocene would be expected to have been.

Clim. Past Discuss., doi:10.5194/cp-2017-21, 2017
Manuscript under review for journal Clim. Past
Discussion started: 24 February 2017

Climate of the Past Discussions

2 Model description

We use the Community Climate System Model version 4 (CCSM4; *Gent et al.* (2011)) for simulating the mid-Pliocene. CCSM4 is a coupled-climate model and is composed of four major components that interact with each other through a flux coupler without flux adjustment. These components are briefly described in this section. CCSM4 has been used in many palaeoclimate studies and it is one of the models to have previously been employed in PlioMIP (*Rosenbloom et al.*, 2013).

2.1 Atmosphere

The atmospheric component in CCSM4 is the Community Atmosphere Model version 4 (CAM4; *Neale et al.* (2013)) which is the sixth generation atmospheric general circulation model developed at the National Center for Atmospheric Research (NCAR). In this version the default dynamical core has changed from a spectral core which was used in CAM3, to a finite volume (FV) dynamical core. The FV core improves tracer transport capabilities over the spectral core and also reduces the surface zonal wind bias that was present in CAM3. In coupled mode, this bias was responsible for resulting in an intensified Antarctic Circumpolar Current (ACC) and excessive transport through the Drake Passage (*Large and Danabasoglu* , 2006). CAM4 also includes changes to the parametrization for deep convection which significantly improves the Madden-Julian Oscillation (*Subramanian et al.*, 2011) and, in coupled CCSM4 mode, the EL Niño-Southern Oscillation (ENSO) variability (*Deser et al.*, 2012). All our simulations are performed on a FV grid with $\sim 1^{\circ}$ horizontal resolution (192 grid cells in the latitude and 288 grid cells in the longitude) with 26 levels in the vertical.

2.1.1 Ocean

The ocean component in CCSM4 is the Parallel Ocean Program, version 2 (POP2; *Smith et al.* (2010)) which was developed at the Los Alamos National Laboratory. It includes significant improvements over version 1 such as the elimination of the cold bias in the equatorial Pacific cold tongue while also increasing the sharpness of the pacific thermocline, and the reduction of the sea surface temperature (SST) and sea surface salinity (SSS) bias along the path of the North Atlantic Drift.

POP2 also comes with a new parametrization for the overflow of density-driven currents over oceanic ridges, such as the overflow of the Nordic Sea waters over the Denmark Strait and the Faroe Bank Channel, and the overflow of dense waters over bottom topography in the Ross Sea and Weddell Sea regions of the Antarctic (*Danabasoglu et al.*, 2010). These overflows are thought to be important to the formation of deep bottom waters (*Briegleb et al.*, 2009). The new parametrization improves the penetration depth of the North Atlantic Deep Water (NADW), but introduces new biases which are worse in coupled simulations compared to uncoupled simulations (*Danabasoglu et al.*, 2010).

An important caveat to be aware of when simulating palaeo climate is that this parametrization is tuned to reproduce, to the extent possible, the observations of the overturning circulation for the present day (such as those

Clim. Past Discuss., doi:10.5194/cp-2017-21, 2017
Manuscript under review for journal Clim. Past
Discussion started: 24 February 2017

obtained by the RAPID array, *Cunningham et al.* (2007)). As such, its impact when included in the simulation of a time period when the ocean bathymetry would have been significantly different remains unclear. Owing to the concern of the biases stemming from this parametrization, and its tuning to the present day, we have chosen to disable the parametrization in all of the simulations for which results will be described in what follows.

In our simulations the ocean model runs on the displaced-pole grid in which the poles of the grid are positioned over Greenland and Antarctica and therefore the ocean does not contain any grid singularities. The grid consists of 60 vertical levels, with 320×384 cells at each level. This comes out to a nominal resolution of $\sim 1^\circ$ although the dimensions of the grid cells are not uniform throughout the oceans.

2.2 Land

The land component in CCSM4 is the Community Land Model version 4 (CLM4; *Lawrence et al.* (2012)). One of the chief deficiencies of version 3 of CLM was its poor representation of the hydrological cycle, which is why version 4 includes a considerably revised hydrology with changes to the surface runoff scheme, the groundwater scheme, soil sub-model hydrology, and revised parameterizations for canopy integration, canopy interception, soil evaporation and frozen soil. These changes have led to notable improvements in soil water content, increased transpiration and photosynthesis and better simulation of the annual cycle of land water storage. Another significant improvement in CLM4 over CLM3 is the addition of a fully prognostic carbon-nitrogen biogeochemical model. This sub-model is able to affect the climate through its control of the seasonal and annual vegetation phenology. The land model runs at the same resolution as the atmosphere model, CAM4, whereas the river transport model which is included with the land model runs at a 0.5° resolution.

2.3 Sea-ice

The sea ice component in CCSM4 is based on the Community Ice Code version 4 (CICE4; *Hunke and Lipscomb* (2006)) developed at the Los Alamos National Laboratory. The main improvement in CICE4 over its predecessor, the Community Sea Ice Model version 5 (CSIM5; *Briegleb et al.*, 2004), is in the shortwave radiative transfer scheme (*Briegleb and Light*, 2007) which now uses the microscopic optical properties of snow, ice and external absorbers (such as black-carbon and dust) to explicitly calculate the multiple scattering of solar radiation in sea ice using a delta-Eddington approximation for the purposes of inferring macroscopic optical properties such as albedo, and transmission. As a result, CCSM4 has a much better representation of sea ice albedo compared to CCSM3-CSIM5 in which the albedo was parametrized using the bulk properties (thickness, temperature etc.) of sea ice and snow. The new radiative transfer scheme has also allowed for the inclusion of a simple melt pond parametrization based upon the surface meltwater flux, and inclusion of the effects of aerosol deposition and cycling. *Holland et al.* (2012) have found that the effects of direct radiative forcing by melt ponds and aerosols on the Arctic sea ice is much higher than on the Antarctic sea ice. The sea ice component operates on the same grid as the ocean component.

Clim. Past Discuss., doi:10.5194/cp-2017-21, 2017
Manuscript under review for journal Clim. Past
Discussion started: 24 February 2017

Climate of the Past Discussions

3 Design of the Numerical Experiments

This section describes the boundary conditions and the initial conditions used in our simulations along with the methodology through which they have been integrated into the CCSM4 model. The simulations are referred to using the nomenclature first employed by *Lunt et al.* (2012) and subsequently adopted with modifications for PlioMIP2 by *Haywood et al.* (2016). In this notation simulations are referred to by the form Ex^c where c is the concentration of atmospheric CO_2 and x represents boundary conditions which have been changed from the pre-industrial (PI) such that x can be absent (for the case in which no boundary conditions have been modified) or it can be either or both 'o' for a change of orography and 'i' for a change of land ice.

Our control and mid-Pliocene simulations were initially integrated for several hundred model years with the diapycnal diffusivity in the ocean, κ, fixed to a constant, depth-independent background value of $0.16cm^2/s$, the modern day pelagic value, and then subsequent integrations of the simulations were continued with κ fixed to the depth-dependent profile that was used in the ocean component, POP1, of the CCSM3 model (*Collins et al.*, 2006). This profile, which we will henceforth refer to simply as the 'POP1 profile', is shown in Supplementary Figure S1 and is characterized by a depth dependent hyperbolic tangent function that gives an upper-ocean κ of $0.16cm^2/s$ and a deep-ocean κ of $1.0cm^2/s$ with the smooth transition between these asymptotic values centered at a depth of 1,000 m. A simulation that has been performed with the POP1 profile will be denoted by appending a P to the name derived using the nomenclature mentioned earlier and will be referred to as the 'POP1 variant'.

The motivation behind the choice of these two diapycnal mixing profiles in the context of palaeoclimate simulations, instead of the more complex and spatially varying profile that is part of CCSM4 has been previously articulated by *Peltier and Vettoretti* (2014). Essentially, the spatially varying component of the CCSM4 mixing field includes a significant contribution from the turbulent mixing that is generated by the flow of the barotropic tide over rough bottom topography and which is tuned in the CCSM4 model for the modern day tidal regime (determined in part by the modern day bathymetry and coastlines). During the mid-Pliocene there were important changes to the coastlines and bathymetry that would have affected regions which are hotspots of tidal mixing in the present day such as, the Maritime Continent, East Pacific Ocean, Labrador Sea, and Denmark Strait and Faroe Bank Channel region in the North Atlantic. Additionally, the elevations of the mid-ocean ridges could have differed from the present day by as much as 500 m (see Figure 7 in *Dowsett et al.*, 2016, comparing PRISM4 bathymetry to modern) due to the influence of dynamic topography (*Moucha et al.*, 2008) which would have also had an important impact on the generation of turbulent mixing. It is for these reasons that we have opted for our choice of the diapycnal diffusivity for the mid-Pliocene ocean, and also for the control simulation oceans so as to facilitate comparison with the mid-Pliocene results without introducing an ambiguity associated with the choice of different mixing schemes. Furthermore, the POP1 and the non-POP1 variants will allow us to assess the degree of impact that diapycnal diffusivity would have on the strength of the meridional overturning circulation.

Clim. Past Discuss., doi:10.5194/cp-2017-21, 2017
Manuscript under review for journal Clim. Past
Discussion started: 24 February 2017

Climate of the Past Discussions
Open Access
EGU

3.1 Control Experiments

We have simulated two control experiments E^{280} and E^{400} (and their POP1 variants $\mathrm{E}^{280}{}_{\mathrm{P}}$ and $\mathrm{E}^{400}{}_{\mathrm{P}}$) with atmospheric CO_2 concentration 280 ppmv and 400 ppmv respectively. Henceforth, we will refer to the former as the PI control, and the latter as the modern control (which resembles modern only inasmuch as the atmospheric CO_2 is close to modern; all other trace gases are identical to the PI control and no urban or agricultural land units are included in the land model.) The orography, bathymetry, land ice and river directions are identical in both controls and have been generated from ETOPO1 (*Amante and Eakins*, 2009). The default modern day orography and bathymetry that is shipped with CCSM4 is generated from the USGS GTOPO30 dataset and our selection of ETOPO1 here is simply for historical reasons. The vegetation, soil and wetland/lakes distribution in the land model is the same as that which is employed in the 1850 configuration in CCSM4 (component set label B_1850_CN). The concentrations of the atmospheric trace gases and orbital parameters are set to those that are prescribed for PlioMIP2 and are listed in Table 1. Both E^{280} and E^{400} are started as CCSM "hybrid runs" from an existing 3,500 year control simulation which was run with an atmospheric CO_2 concentration of 280.4 ppmv.

3.2 Pliocene Experiments

We report on two PlioMIP2 mid-Pliocene experiments namely the Core simulation $\mathrm{E}oi^{400}$ and the Tier 1 simulation $\mathrm{E}oi^{450}$. In keeping with the notation discussed above, both these simulations include the modified orography (and bathymetry) and land ice specified by the PLioMIP2 "enhanced" boundary conditions described in *Dowsett et al.* (2016). The POP1 variants of these simulations have also been performed. Additional PlioMIP2 mid-Pliocene experiments, and experiments (not included in the PlioMIP2 experiment list) exploring the sensitivity of the climatology to variations in PlioMIP2 boundary conditions were also performed, but the results of these simulations will not be discussed in the present paper. In order to keep our discussion concise and straightforward, we will focus only on the 400 ppmv Pliocene simulations ($\mathrm{E}oi^{400}$ and $\mathrm{E}oi^{400}{}_{\mathrm{P}}$) and will refer to results from the 450 ppmv simulations only in selected discussions. The following sub-sections describe the process through which the PlioMIP2 enhanced boundary conditions have been integrated into the CCSM4 model.

3.2.1 Orography and the Atmosphere Model

The orography, or above sea-level topography which includes the topography of ice-sheets, appears as a boundary condition primarily in the atmospheric component of the coupled model where this field is ingested by the model in the form of the surface geopotential height field. Another application of orography is in the generation of the global dataset of river direction vectors which is used by the land model and is discussed further below. Following the anomaly method (*Haywood et al.*, 2016), we have first computed the anomaly between the PlioMIP2 mid-Pliocene orography and the PlioMIP2 modern orography and then superimposed this anomaly, shown in Figure 1, on our local modern orography. This method leads to subtle differences between the resulting land-sea mask (LSM) and the LSM

Clim. Past Discuss., doi:10.5194/cp-2017-21, 2017
Manuscript under review for journal Clim. Past
Discussion started: 24 February 2017

prescribed in PlioMIP2 and therefore in an effort to maintain the integrity of the PlioMIP2 LSM, we conditionally overwrite the orography of any grid cell where the LSM differs from that described by PlioMIP2.

3.2.2 Bathymetry and the Ocean Model

The vertical levels in the POP2 ocean model are referred to as "KMT levels" whose values are in the range 1-60. Prescribing the mid-Pliocene bathymetry thus requires generating a two-dimensional array containing the KMT levels of each ocean grid cell. An initial KMT field is easily obtained by using the POP2 model's ancillary scripts and the PlioMIP2 mid-Pliocene bathymetry. However, this raises a number of issues which need to be addressed. These issues fall into two categories, (i) conflict between the LSM on the displaced dipole ocean grid and the PlioMIP2 LSM, particularly along straits and regions that contain archipelago or complex coastlines, and (ii) issues pertaining to the requirements of the ocean model such as the minimum KMT level, and the minimum width of narrow straits, in terms of the number of grid cells, which is required to permit flow through them.

We have created a suite of graphical tools to enable the targeted editing of boundary condition data products for CCSM4, such as editing the KMT levels. Figure 2 shows a screen-shot from one of the tools - KMTEditor which is seen here zoomed over a region of the North Atlantic. The thick black rectangle is a cursor over a pixel and the pixels with thin black borders indicate those cells whose values have been edited. The ocean model is initialized from a state of rest with modern day temperature and salinity derived from *Levitus and Boyer* (1994). No adjustment was made to the global salinity for the +25 m mid-Pliocene sea level because any applicable adjustment would be negligible. In comparison, for the case of the Last Glacial Maximum, at which time the globally averaged sea level was lower than present by 120 m, coupled-climate simulations increase the ocean salinity by 1 PSU compared to modern to account for the reduced volume of the oceans (see *Vettoretti and Peltier*, 2013; *Peltier and Vettoretti*, 2014).

3.2.3 Land Model and River Transport Model

The land model is capable of dynamically predicting vegetation types as a response to evolving local climate. However, the simulations described here are run with the dynamical vegetation scheme turned off. Instead, we prescribe the mid-Pliocene vegetation reconstruction by *Salzmann et al.* (2008) which was also used in PlioMIP. This reconstruction is generated using the BIOME4 scheme (*Prentice et al.*, 1992) and is available either as a 28-type 'biome' dataset or a 9-type 'mega-biome' dataset. Because of the uncertainties that are associated with vegetation reconstructions so far back in time, we use the mega-biome dataset instead of the biome dataset so as to minimize error.

The CLM4 model represents vegetation in terms of 17 plant functional types (PFTs) and is able to represent multiple PFTs and land units within a grid cell using a sub-grid hierarchy. In order to be able to use the *Salzmann et al.* (2008) reconstruction, the mega-biome types have to be mapped into PFTs. We have generated one such mapping by projecting the modern day mega-biome types onto the modern day PFTs. Such a map turns out to be a one-to-many map but it is readily accommodated in CLM4 because of its ability to represent multiple PFTs per grid cell. The detailed properties of this mapping are described in the supplementary materials.

Clim. Past Discuss., doi:10.5194/cp-2017-21, 2017
Manuscript under review for journal Clim. Past
Discussion started: 24 February 2017

Climate of the Past Discussions

The soil color was kept fixed to modern (*Lawrence and Chase*, 2007). The direction vectors for river routing were generated from the gradient of the topography. These were inspected and edited manually using another graphical tool to ensure that all rivers reach the oceans (or an inland sea) and that there are no river loops which would prevent some fresh water from reaching the oceans and consequently leading to salinity drift in the ocean.

4 Results and Discussion

We present the results from our experiments organized into seven individual sub-sections. The discussion is based on the climatology that is simulated in our experiments for the mid-Pliocene, and the control experiments. These climatologies represent the average over 30 model years which is the required averaging duration that was agreed upon at the PlioMIP2 workshop in Leeds in 2016. Only climatologies of the POP1 variants of the simulations will be discussed in what follows.

4.1 Model Evolution

The objective of PlioMIP2 is to simulate the equilibrium climate of the typical interglacial in the mid-Pliocene. Therefore, the climate simulations need to be run for a length of time that is sufficiently long to ensure that the various components of the coupled-model system have come into equilibrium, in particular, in order to ensure that the ocean, which takes much longer than the atmosphere to equilibrate, has also reached an equilibrium state. Figure 3 and Figure 4 show the evolution of the ocean temperature in our simulations, and Figure 5 shows the evolution of the surface air temperature (SAT). In these figures, a "fork" in a timeseries denotes the branching of the POP1 variant of that experiment (see Section 3) from the constant kappa variant. In all cases the original simulations were also allowed to evolve for considerable time. The total number of model years for which each of our simulations has been run and the top of the atmosphere (TOA) energy imbalance over the last 30 years is listed in Table 4. All simulations have very low TOA energy imbalance indicating that the models are in very close to statistical equilibrium states.

It is observed that while the SSTs (Figure 3a) in all models have come into equilibrium, the deep ocean is continuing to warm (Figure 3d). It is also seen that introduction of the POP1 profile for κ leads to greater exchange of heat between the upper ocean and the deeper ocean as expected on physical grounds. This increases the rate of warming for the middle and the lower ocean and decreases the rate of warming for the upper ocean. When the entire ocean is considered as a whole, all models continue to take up heat and their individual warming trends are remarkably linear (Figure 4.) The PI control shows the slowest rate of warming ($0.04\,^{\circ}\mathrm{C/century}$), even after the introduction of the POP1 profile for κ, which is due to the fact that this control run was initialized from an existing 3,500 year control and integrated for a further 1,700 years which has given the deep ocean sufficient time to come into equilibrium. The modern control is warming at a slightly faster rate of $0.07\,^{\circ}\mathrm{C/century}$. The $\mathrm{E}oi^{400}$ and $\mathrm{E}oi^{450}$ mid-Pliocene simulations are warming at rates of $0.07\,^{\circ}\mathrm{C/century}$ and $0.08\,^{\circ}\mathrm{C/century}$ respectively at the end of 2,500 years of integration.

Clim. Past Discuss., doi:10.5194/cp-2017-21, 2017
Manuscript under review for journal Clim. Past
Discussion started: 24 February 2017

Climate of the Past Discussions

4.2 Surface Air Temperature

The mean annual surface air temperature (MASAT) anomalies for the $\mathrm{E}oi^{400\mathrm{P}}$ mid-Pliocene simulation compared to both our control simulations are shown in Figure 6. A polar stereoscopic projection is employed for these graphics because the SAT anomalies exhibit distinct spatial features only in the high latitudes. Compared to the PI, the mid-Pliocene temperatures at both poles are much higher. The pattern in the northern hemisphere bears resemblance to the polar amplification that is observed in contemporary measurements of surface temperatures. However, the mid-Pliocene differs from PI (and modern) in the land-sea mask, ice-sheet configuration and vegetation. Because of these changes, the amplification near the poles during the mid-Pliocene is expected to include feedback mechanism which are not active in the present day.

The MASAT anomaly compared to modern is shown in Figure 6b. Because both the mid-Pliocene and the modern experiments have the same atmospheric CO_2 concentration, this anomaly to a good approximation, excludes the warming signal that would arise from differences in atmospheric CO_2 , such as was the case for the MASAT anomaly as compared to pre-industrial conditions. Therefore the MASAT anomaly with respect to modern conditions represents the impacts of other changes related to the mid-Pliocene boundary conditions and the feedbacks associated with those changes. Naturally, the amplitude of warming is expected to be reduced compared to what would be obtained in comparison to PI conditions. The zonal averages of both MASAT anomalies (Figure 8) demonstrates that the anomaly compared to modern is about $1\,^{\circ}\mathrm{C}$ lower than the anomaly compared to PI throughout the tropics and sub-tropics. However, at high latitudes, we begin to see a difference between the two anomalies - while in the southern hemisphere the difference between the anomalies as compared to both control simulations continues to remain at a level of approximately $1\,^{\circ}\mathrm{C}$, peaking at $\sim 2\,^{\circ}\mathrm{C}$ around $70^{\circ}\mathrm{S}$, in the northern hemisphere the difference between the two anomalies diverges rapidly. The larger anomaly with PI appears to be due to the 120 ppmv CO_2 difference between the mid-Pliocene and PI and to the dramatic difference between the northern hemisphere LSM.

The globally averaged MASAT is $16.8\,^{\circ}\mathrm{C}$ for model $\mathrm{E}oi^{400\mathrm{P}}$ and $17.3\,^{\circ}\mathrm{C}$ for model $\mathrm{E}oi^{450\mathrm{P}}$ (see Table 2). The 400 ppmv mid-Pliocene simulation is $3.8\,^{\circ}\mathrm{C}$ warmer than the PI, and the 450 ppmv mid-Pliocene simulation is $4.3\,^{\circ}\mathrm{C}$ warmer. These values are larger than the magnitude of the anomaly predicted by every model that has been exercised previously in the context of the PlioMIP program (*Haywood et al.*, 2013) and double the anomaly that *Rosenbloom et al.* (2013) found ($1.86\,^{\circ}\mathrm{C}$) using CCSM4. Our simulated anomaly is also much higher than that found by *Kamae et al.* (2016) ($2.4\,^{\circ}\mathrm{C}$) using the PlioMIP2 boundary conditions and the MRI-CGGM2.3 coupled climate model. A likely explanation as to why their anomaly is lower than ours could be due to their choice of the 'standard' boundary conditions set which does not require changes to the land-sea mask in the model. A more likely explanation of the difference, however, is simply that the relatively short integration length of 500 years would not have been sufficient to enable the ocean in their model from reaching a state of quasi-equilibrium.

The Equilibrium Climate Sensitivity (ECS) of the planet calculated based our mid-Pliocene simulations is also given in Table 2. The ECS from our 400 ppmv mid-Pliocene experiment is $7.4\,^{\circ}\mathrm{C}$ per doubling of CO_2 . Although this

Clim. Past Discuss., doi:10.5194/cp-2017-21, 2017
Manuscript under review for journal Clim. Past
Discussion started: 24 February 2017

Climate of the Past Discussions

number is fairly high, it agrees well with the $7.1 \pm 1.0 - 9.7 \pm 1.3$ range of estimates that *Pagani et al.* (2010) inferred using proxy based methods. Our estimate for the ECS is double that obtained using CCSM4 for PlioMIP of $3.51^{\circ}\mathrm{C}$, and significantly higher than the PlioMIP multi-model mean of $5.01^{\circ}\mathrm{C}$.

Both of our mid-Pliocene simulations show the greatest warming during the months of JJA and least warming during the months of DJF (Table 3). The warming during JJA is more than a degree greater than that during DJF for both mid-Pliocene models and compared against both of our controls. In fact, while the JJA-DJF temperature difference in our control simulations are $\sim 3.5^{\circ}\mathrm{C}$ the difference is $\sim 4.7^{\circ}\mathrm{C}$ in the mid-Pliocene simulations. This represents an increase in seasonality in the mid-Pliocene over that under either pre-industrial or modern conditions.

In Figure 7 we show the northern hemisphere SAT anomalies in $\mathrm{E}oi^{400}\mathrm{P}$ for JJA and DJF which captures this seasonality. The first row shows the anomalies relative to the PI and the second row shows the anomalies relative to modern. The increase in seasonality in the mid-Pliocene is readily apparent, especially in comparison to modern conditions such that the Pliocene winter (summer) is colder (warmer) than modern over land. The significant and widespread cooling of the mid-Pliocene winter compared to modern is not easily understood, although it is not unlike the temperature trend that has been observed in recent decades (*Cohen et al.*, 2013; *Overland et al.*, 2011; *Sun et al.*, 2016). A comprehensive examination of the seasonality, and of the cooling during the winter will be the subject of a further publication to be presented elsewhere.

4.3 Precipitation

The anomaly of the mid-Pliocene annual precipitation compared to our two control simulations is shown in Figure 9. We see the presence of a strong double ITCZ which is a recognized problem with CAM4 (*Gent et al.*, 2011). The anomaly is larger with respect to the PI than it is with respect to modern conditions. This is expected as the Pliocene atmosphere is much warmer than the PI owing to greater atmospheric CO_2 , whereas the atmosphere in the modern control has the same CO_2 concentration as the Pliocene. Despite the differences in the magnitude of the anomalies, the broad features remain the same. The precipitation increases over mountain belts such as the Andes, the Himalayas and the Tibetan plateau are due to the increased mid-Pliocene orography of these regions (Figure 1) and to the higher moisture content of the air rising above these mountain belts.

4.4 Ocean Temperature

Figure 10 shows the mid-Pliocene SST as well as the SST anomalies compared to the PI control and the modern control. Our simulation is characterized by the existence of a fairly extensive expansion of the warm pool in the mid-Pliocene, a feature whose existence has been previously suggested on the basis of proxy based reconstructions of SSTs (*Brierley et al.*, 2009; *Dowsett et al.*, 2012; *Fedorov et al.*, 2012). The blue and the red contour lines in Figure 10a show the extent of $30^{\circ}\mathrm{C}$ and $31^{\circ}\mathrm{C}$ waters of the equatorial warm pool. Such warm waters are not present in the PI control simulation for which the temperature in the equatorial warm pool is $1.5 - 2^{\circ}\mathrm{C}$ lower than the mid-Pliocene. Warm waters are also present at high latitudes in the North Atlantic, and in the Southern Ocean, where the SST

Clim. Past Discuss., doi:10.5194/cp-2017-21, 2017
Manuscript under review for journal Clim. Past
Discussion started: 24 February 2017

Climate of the Past Discussions

anomalies show amplified warming compared to the rest of the ocean. The related shift in the east-west temperature gradient across the equatorial Pacific is expected to have a (perhaps significant) impact upon the ENSO process, an impact that will be discussed in detail elsewhere.

Another way through which the mid-Pliocene ocean can be compared to our two controls is through the meridional profile of zonal-mean SST, which is shown in Figure 11 for the Atlantic-Arctic basin and the Southern-Indian-Pacific basin. In both basins, the mid-Pliocene ocean is warmer than the PI by at least $2.5 - 3.5\,^{\circ}\mathrm{C}$, and warmer than the modern by at least $1 - 2\,^{\circ}\mathrm{C}$. The largest anomalies occurs in the 45°N-65°N region of the Atlantic where most of the NADW forms.

The data points in Figure 11 show proxy based estimates for the mid-Pliocene SST that has been compiled by *Brierley et al.* (2009). While plotting these estimates we have retained the temporal corrections, whenever applicable, that *Brierley et al.* (2009) have calculated, but we do not apply the location corrections which the authors had used to adjust the raw data to represent the mid-Pacific. We find that our simulated meridional SST profile is in rather good agreement with the limited number of data points that are available. A disagreement is seen near the equator in the Indo-Pacific basin where the Mg/Ca and alkenone based estimates for the SST are $\sim 2\,^{\circ}\mathrm{C}$ lower than our simulated SST. The proxy estimates in fact match batter to the modern control than to the mid-Pliocene. However, this is in precise agreement with what *O'Brien et al.* (2014) have recently argued regarding the ineptitude of Mg/Ca and Alkenone based proxies to capture the significantly warmer temperatures in this region. Specifically, they argue that the insensitivity of alkenone proxies to temperatures $> 29\,^{\circ}\mathrm{C}$ and the dependence of the Mg/Ca calibration to seawater Mg/Ca ratios fail both proxies when it comes to recording the warmer temperature waters during the mid-Pliocene, which has lead to speculations of 'thermostat like mechanisms' that might have limited the warm pool temperatures during the Pliocene. Using the TEX_{86} proxy as well as a revised calibration of Mg/Ca proxy *O'Brien et al.* (2014) argue that the equatorial warm pool temperatures were about $2\,^{\circ}\mathrm{C}$ warmer than preset day, a suggestion with which our simulated results agree.

We have also compared the simulated mid-Pliocene SST to the large compilation of SST estimates that has been produced in the context of the PRISM3 program (*Dowsett et al.*, 2010). Before we discuss this comparison it needs to be noted that the PRISM3 reconstruction was generated for the original PlioMIP program in which the aim was to simulate the average climate of the warm intervals in a 300,000 year time slab from ~ 3.3 to 3 millions years ago and therefore the PRISM3 boundary conditions and the SST reconstructions are an average over that time period. The PRISM3 dataset is therefore not strictly applicable to PlioMIP2 in which the focus is on a time-slice centered on the single interglacial peak at MIS KM5c. However, since the revised dataset that will be eventually applicable to PlioMIP2 is not yet available, we will be comparing our results to PRISM3.

Figure 12 shows the PRISM3 estimate for the mid-Pliocene SST anomalies (compared to PI) categorized into three confidence levels (*Dowsett et al.*, 2012) - Very High, High and Medium confidence. There are roughly 100 sites in the PRISM3 dataset distributed over all ocean basins and which have been arranged as a function of latitude in the figure. The data indicates that the mid-Pliocene ocean was on average a few degrees warmer than the present day and that

Clim. Past Discuss., doi:10.5194/cp-2017-21, 2017
Manuscript under review for journal Clim. Past
Discussion started: 24 February 2017

Climate of the Past Discussions

the warming was particularly pronounced in the high-latitudes of the northern hemisphere. The SST anomalies at PRISM3 sites obtained from our mid-Pliocene simulations $\mathrm{E}oi^{400\mathrm{P}}$ and $\mathrm{E}oi^{450\mathrm{P}}$ are shown on Figure 12b in blue and green dots respectively. Both simulations are able to capture the high-latitude warming in the northern hemisphere, except at the locations of the most northern data points, whose reliability has recently been called into question in the Pliocene community. Our mid-Pliocene ocean is warmer than the data suggests in the Southern Ocean but the differences are not extreme.

Also shown on Figure 12a are the mid-Pliocene SST anomalies obtained with CCSM4 (black dots; *Rosenbloom et al.* (2013)) using the PRISM3 boundary conditions (*Sohl et al.*, 2009) for the PlioMIP program, and the multi model mean (MMM) from PlioMIP (black squares). With the PRISM3 boundary conditions, the original CCSM4 simulation had difficulty in simulating the northern hemisphere high-latitude warming. The response of the model is very flat across all latitudes. The MMM from PlioMIP similarly did not simulate any enhanced warming in the high-latitudes. However, with the PRISM4 boundary conditions the CCSM4 model is seen to very well simulate the amplification near the poles when the model is run to near statistical equilibrium (Figure 12b). It is beyond the scope of this paper to address the question as to what specific mechanisms might be contributing to this warming. It is also possible that answering this question will require the full set of sensitivity studies (or perhaps more) that has been proposed for PlioMIP2 (*Haywood et al.*, 2016), which would require significant computational resources.

4.5 Meridional Overturning Circulation

In Figure 13 we show the evolution of the Atlantic Meridional Overturning Circulation (AMOC) maximum in our simulations. The AMOC in all our simulations appear to have reached equilibrium. The mean state of the AMOC maximum for each simulation over the 30 year climatology is cataloged in Table 4. It is seen that across all simulations the AMOC is ~ 2 Sv stronger in the variants which have the POP1 diffusivity profile compared to the variants that employs only the background pelagic value of the diapycnal diffusivity. The dependence of the AMOC on the nature of vertical mixing is expected, and therefore it is something to be kept in mind when comparing AMOCs from different models, each with their own vertical mixing schemes (*Zhang et al.*, 2013b). Additionally, the AMOC shows more variability in simulations with the POP1 mixing profile.

The strength of the AMOC in the PI control is 20 Sv and 21.5 Sv for simulations E^{280} and $\mathrm{E}^{280\mathrm{P}}$ respectively, and in the modern control simulations E^{400} and $\mathrm{E}^{400\mathrm{P}}$ the AMOC strengths are 21.9 Sv and 24.2 Sv. Our climatological estimates of the PI AMOC are in satisfactory agreement with the 17.2 Sv that has been estimated over a short time span (years 2004 - 2012) by *McCarthy et al.* (2015) using measurements obtained from the RAPID monitoring array.

Several different proxies on the basis of which it has been argued that one may infer the strength of NADW or Antarctic Bottom Water (AABW) formation have been invoked to argue for a more vigorous mid-Pliocene AMOC – sometimes called the "super conveyor" – compared to the present day. These include arguments from comparisons of mid-Pliocene benthic $\delta^{13}\mathrm{C}$ values in ocean basins to modern day values (*Billups et al.*, 1997; *Ravelo and Anderson*, 2000; *Raymo et al.*, 1996), measurements of Nd and Pb isotope composition recorded in ferromanganese crusts

Clim. Past Discuss., doi:10.5194/cp-2017-21, 2017
Manuscript under review for journal Clim. Past
Discussion started: 24 February 2017

Climate of the Past Discussions

and nodules (*Frank et al.*, 2002), oceanic carbonate dissolution history (*Frenz et al.*, 2006) and reconstructions of past marine ice-sheet extents in the Ross Ice Shelf regions (*McKay et al.*, 2016). However, similar to our own findings that we will report below, coupled climate models have not been able to reproduce such invigorated AMOC in the mid-Pliocene (*Haywood and Valdes* , 2004; *Zhang et al.*, 2013b), and indeed for end-of-century which like the mid-Pliocene would be a warm climate, multi-model projections show a very-high likelihood of a reduction in the strength of the NADW cell (*Collins et al.*, 2013).

The inability of models in the PlioMIP project to simulate an energized AMOC (*Zhang et al.*, 2013b) coincides with the additional failure of these models to simulate the northern hemisphere SST amplification that proxy records suggest (Figure 12a). It has therefore been previously argued (*Haywood et al.*, 2016; *Hu et al.*, 2015) that the closure of the Bering Strait (in PlioMIP2) could lead to larger AMOC and consequently greater oceanic heat transport to higher latitudes in the North Atlantic. If this were to happen, then that would not only reconcile the model predictions with SST proxies, but also with the proxies that suggest an intensified AMOC. Recently, *Hu et al.* (2015) reported on the effects of the closure of the Bering Strait on AMOC strength and the meridional heat transport using CCSM3 and CCSM2 under present, 15 thousand years before present and 112 thousand years before present boundary conditions. They found that under all these conditions, i.e. regardless of the background climate state, and for both models the closure of the Bering Strait resulted in a strengthening of the AMOC by $\sim$ 2-3 Sv.

We find that the AMOC in our 400 ppmv and 450 ppmv mid-Pliocene simulations are almost identical and their strengths are only 2-3 Sv higher than PI control (Figure 13). This represents an increase of the mid-Pliocene AMOC by just 10% over the PI AMOC and therefore does not lend support to the idea of a significantly intensified AMOC during the mid-Pliocene. This increase is comparable to the increase that has been estimated by *Hu et al.* (2015) to result from the closure of the Bering Strait and would therefore lead one to speculate that the stronger AMOC in our mid-Pliocene simulations is the result of the closure of the Bering Strait. However, this argument is complicated by the fact that the AMOC in the 400 ppmv modern control, which like the PI control is characterized by an open Bering Strait, is stronger than that in the mid-Pliocene simulations. Additionally, our 400 ppmv Pliocene AMOC is weaker than that simulated with the CCSM4 model in PlioMIP (which had an open Bering Strait, *Zhang et al.*, 2013b), although this could be due to the much shorter model run (550 years) on the basis of which the PlioMIP CCSM4 diagnostic was computed. Therefore, it is presently not possible to conclude that the marginal strengthening of the AMOC seen in our mid-Pliocene simulations is due to the closing of the Bering Strait.

4.6 Meridional Heat Transport

The atmosphere and the ocean are together responsible for transporting the excess heat that accumulates near the equator to the high latitudes, where this heat can be radiated to space in the form of longwave radiation, thereby helping to maintain an equilibrium climate. Under present day conditions the maximum transport of heat poleward is $\sim 5.5\,\mathrm{PW}$ that peaks at $30°$- $40°$ latitudes in each hemisphere (*Trenberth and Carson*, 2001). The atmosphere dominates the heat transport poleward of the sub-tropics and the peak transport of heat is $\sim 5\,\mathrm{PW}$ at $40°$ latitudes.

Clim. Past Discuss., doi:10.5194/cp-2017-21, 2017
Manuscript under review for journal Clim. Past
Discussion started: 24 February 2017

Climate of the Past Discussions

By comparison, the ocean carries much less heat and dominates only in the deep-tropics. The maximum heat transported by the ocean is just under $2\,\mathrm{PW}$. These characteristic of the present day meridional heat transport are well represented in our control simulations (Figure 14).

Figure 14 shows that the total meridional heat transport in our $\mathrm{E}oi^{400}\mathrm{P}$ mid-Pliocene simulation is lower than both the PI and modern controls. The reduction in the transport of heat is seen in both the atmosphere and the ocean. The atmospheric heat transport (AHT) in all our simulations (mid-Pliocene and controls) is essentially identical throughout the tropics, the sub-tropics and the southern hemisphere. The only notable difference arises in the mid-to-high latitudes of the northern hemisphere where the mid-Pliocene AHT is lower than both controls (Figure 14a,c). A very small difference in AHT between the mid-Pliocene and the control is also noticed close to $65°\mathrm{S}$ which might be due to the substantial differences in topography and grounded ice-sheets between the two simulations at this latitude.

The reduction in the oceanic heat transport (OHT) in the mid-Pliocene is primarily due to the reduction in OHT in the Indo-Pacific basin (Figure 14b,d). It is likely that this reduction can be attributed to the closing of the Bering Strait. *Hu et al.* (2015) have shown that closing the Bering Strait can lead to a decrease in the northward heat transport in the North Pacific by $\sim 10\% - 15\%$ compared to the case with an open Bering Strait. We find that the North Pacific OHT in our mid-Pliocene simulation (which has a closed Bering Strait) is lower than both our control simulations (with open Bering Strait) by $\sim 20\% - 25\%$. Although a comparison between our mid-Pliocene simulations and our control simulations is not the same as comparing two simulations with identical boundary conditions save for the differences along the Bering Strait, as *Hu et al.* (2015) have done, our analysis suggest that their results regarding the impact of the closing of the Bering Strait on the North Pacific OHT is a robust response of the climate system that persists even when there are other differences in boundary conditions.

We find that the southward OHT in the South Pacific during the mid-Pliocene is also reduced compared to the PI. This, however, is in contrast to the consistent increase in the southward OHT in the South Pacific that *Hu et al.* (2015) found as a consequence of the closure of the Bering Strait. This suggests to us that the difference in the atmospheric radiative forcing, and the geographical changes between the mid-Pliocene and the PI control have had an impact on the southward OHT in the South Pacific, in addition to that which would be expected from the analysis of *Hu et al.* (2015). However, we have to be cautious concerning this comparison, as the simulated differences could also be due to the differences between the ocean components in these versions of CCSM. Both CCSM2 and CCSM3 use POP1 as their ocean model, whereas CCSM4 uses the POP2 ocean model.

The OHT in the Atlantic basin during the mid-Pliocene is only marginally higher, by $\sim 3\%$, than the PI. This increase is substantially less than the $\sim 10\%$ increase in the strength of the AMOC. The mid-Pliocene Atlantic OHT is also nearly identical to the modern control despite geographical differences between the two cases. In fact, in the latitude range $50°\mathrm{N}$-$70°\mathrm{N}$ the Atlantic in the modern control is transporting more heat that the Atlantic in the mid-Pliocene. This makes it further difficult to assess whatever impact the closed Bering Strait might be having on the

Clim. Past Discuss., doi:10.5194/cp-2017-21, 2017
Manuscript under review for journal Clim. Past
Discussion started: 24 February 2017

mid-Pliocene climate through the reorganization of oceanic heat transport, and points to the possibility of increasing meridional heat transport in the Atlantic sector without the need for closing the Bering Strait.

Finally, we note the presence of what appears to be a local Bjerknes compensation around $65°$S latitude in our 400 ppmv mid-Pliocene simulation (Figure 14a,c). In the vicinity of this latitude, the mid-Pliocene AHT is reduced compared to both the controls. It is then left up to the ocean to transport the excess heat southward of this latitude and consequently the OHT becomes greater than that in the controls. This compensation ensures that there is no anomalous change in the net meridional heat transport near this latitude.

4.7 Sea-ice

The mid-Pliocene sea ice is considerably reduced in extent during both boreal and austral winters compared to PI (Figure 15). In the northern hemisphere the greatest loss in sea ice occurs (besides the Hudson Bay, which is expected not to be present during the mid-Pliocene) in the Labrador Sea and the Greenland and Norwegian Seas in the Atlantic sector, and in the Barents and Kara Seas in the Arctic sector. The reduction in northern hemisphere sea ice is particularly pronounced in the summer months to the extent that the Arctic can be considered ice-free.

Sea ice is uniformly reduced along the coastlines of Antarctica during the austral winter. The largest reduction in sea ice is seen in the Weddell Sea and off the coast of Queen Maud Land and Wilkes Land. The sea ice is most concentrated in the vicinity of the mid-Pliocene Antarctic archipelago and in the region presently occupied by the Filchner-Ronne ice shelf. The presence of the archipelago has allowed for the ice that today forms in the Bellingshausen and Amundsen Seas to move closer towards the pole and therefore lead to a poleward retreat of the ice margin. In austral summer the only concentration of sea ice is in the archipelago while the rest of the Antarctica coastline is largely ice-free.

5 Conclusions

In this paper we have described the implementation of revised boundary conditions for the mid-Pliocene epoch in the CCMS4 coupled climate model and employed the new structure in the reconstruction of the mid-Pliocene climate conditions. We have performed two mid-Pliocene experiments, the core experiment denoted $\mathrm{E}oi^{400}$ and the Tier 1 experiment denoted $\mathrm{E}oi^{450}$, along with the core control experiments E^{280} and the Tier 2 control experiment E^{400}. In addition, we have two versions of these simulations which are differentiated by the ocean's vertical profile of mixing. The first version has a constant (pelagic) value of diapycnal diffusivity throughout the ocean. The second version has its mixing profile fixed to that used by the ocean component POP1 of the CCSM3 model. The discussions and analysis in this paper are based on the climatology that is simulated by the second version of the experiments.

We find that the PRISM4 boundary conditions mandated in PlioMIP2 lead to greater warming in the mid-Pliocene, and in particular enhanced warming at high-latitudes compared to that inferred using the same CCSM4 model and the PRISM3 boundary conditions from the original PlioMIP. The simulated 400 ppmv mid-Pliocene climate has a global

Clim. Past Discuss., doi:10.5194/cp-2017-21, 2017
Manuscript under review for journal Clim. Past
Discussion started: 24 February 2017

Climate of the Past Discussions
Open Access
EGU

MASAT that is $3.8\,^{\circ}\mathrm{C}$ higher than the PI control and $1.8\,^{\circ}\mathrm{C}$ higher than the modern day control. These anomalies are larger than the anomalies predicted by every model previously exercised in PlioMIP and more than double the anomaly that was obtained with CCSM4 in this context (*Haywood et al.*, 2013), demonstrating that the changes to the boundary conditions have had considerable impact on the climate, but also we expect that it is important that such integrations need to be run to statistical equilibrium. In addition, we find that globally averaged temperature difference between the seasons JJA and DJF has increased during the mid-Pliocene compared to both the PI and the modern controls. While the JJA-DJF temperature difference in both of our controls is $\sim 3.5\,^{\circ}\mathrm{C}$ the difference increases to $\sim 4.7\,^{\circ}\mathrm{C}$ in the mid-Pliocene.

The mid-Pliocene ocean that we have simulated is characterized by (i) a fairly expansive warm pool where the temperatures are $1.5-2\,^{\circ}\mathrm{C}$ warmer than the PI, and by (ii) elevated levels of warming at high-latitudes in the Southern Ocean and the North Atlantic. The SST anomalies with respect to PI agree rather well with the proxy inferred SST anomalies compiled for the PRISM3 reconstruction. Both the 400 ppmv and 450 ppmv mid-Pliocene simulations are able to capture the mid-to-high latitude warming that is seen in the PRISM3 dataset. The agreement between the results of our simulations with the new boundary conditions, and the PRISM3 dataset is much better than that which was possible with any of the models in the original PlioMIP (*Dowsett et al.*, 2013). The caveat to our present result is that the PRISM3 SST reconstruction was generated for the original PlioMIP program in which the aim was to simulate the average climate of the warm intervals in a 300,000 year time slab from ~ 3.3 to 3 millions years ago and therefore the PRISM3 boundary conditions and the SST reconstructions are an average over that time period. The PRISM3 dataset is therefore not strictly applicable to PlioMIP2 in which the focus is on a time-slice centered on the single interglacial peak at MIS KM5c. However, the revised dataset that will be applicable to PlioMIP2 is not yet available. When the dataset has been made available, we will revisit this data-model comparison.

The larger warming that is seen in both SAT and SST in our simulations at high-latitudes is accompanied by a decrease in the net meridional heat transport compared to that in either of our controls. The reduced meridional heat transport is the result of reduction in both the atmospheric and oceanic transports. Partitioning of the OHT into contributions from the major oceanic basins shows that the northward transport of heat is greatly reduced in the Indo-Pacific basin. In the Atlantic basin, the meridional transport of heat is only marginally increased ($\sim 3\%$) compared to the PI control, while compared to the modern control, it is either identical or in the high northern latitudes, lower than the control. This suggests that the amplified warming at the high latitudes in the mid-Pliocene, inferred from proxies and supported by our simulations, could have more to do with the local positive feedback processes activated by the changes in geography, ice sheets and vegetation, than with the increased northward transport of heat.

Lastly, we note that our simulations do not support the case for a mid-Pliocene AMOC which is substantially stronger than in the PI control. The existence of a stronger AMOC has been argued from various proxy based inferences (*Billups et al.*, 1997; *Ravelo and Anderson*, 2000; *Raymo et al.*, 1996; *Frank et al.*, 2002; *Frenz et al.*, 2006; *McKay et al.*, 2016) and it has been considered as a possible remedy to the inability of previous climate models to simulate an amplified high-latitude mid-Pliocene warming. Our mid-Pliocene AMOC is only $\sim 10\%$ stronger than the

Clim. Past Discuss., doi:10.5194/cp-2017-21, 2017
Manuscript under review for journal Clim. Past
Discussion started: 24 February 2017

PI AMOC and slightly weaker than the AMOC in modern control (Table 4; Figure 13). It has been argued that the closed Bering Strait in the latest boundary conditions should lead to a stronger AMOC (*Haywood et al.*, 2016; *Hu et al.*, 2015). Although our mid-Pliocene AMOC is indeed stronger than the PI AMOC, the fact that it is also weaker than the modern control AMOC makes it difficult to support the idea that a closed Bering Strait would necessarily lead to a stronger AMOC.

Acknowledgements. Computations were performed on the TCS supercomputer at the SciNet HPC Consortium. SciNet is funded by: the Canada Foundation for Innovation under the auspices of Compute Canada; the Government of Ontario; Ontario Research Fund - Research Excellence; and the University of Toronto. We are grateful to Dr. Guido Vettoretti for guiding DC through the intricate process of implementing boundary conditions for palaeoclimate simulations with CESM. We are also grateful to NCAR for organizing the annual CESM tutorial, one of which was attended by DC, with partial support from NCAR. We would also like to thank Dr. Bette Otto-Bliesner for funding a short visit for DC to NCAR which allowed him to understand more about the CESM model and helped him to implement the mid-Pliocene boundary conditions. DC is also very grateful to The Centre for Global Change Science, University of Toronto, which has funded multiple trips to conferences and workshops related to the work described in the paper. The research of WR Peltier at the University of Toronto is funded by NSERC Discovery Grant A9627.

Clim. Past Discuss., doi:10.5194/cp-2017-21, 2017
Manuscript under review for journal Clim. Past
Discussion started: 24 February 2017

Climate of the Past Discussions

References

Alley, R. B., Clark, P. U., Huybrechts, P. and Joughin, I.: Ice-Sheet and Sea-Level Changes, Science, 310, 456–460, 2005.

Amante, C. and Eakins, B.W.,: ETOPO1 1 Arc-Minute Global Relief Model: Procedures, Data Sources and Analysis. NOAA Technical Memorandum NESDIS NGDC-24. National Geophysical Data Center, NOAA. doi:10.7289/V5C8276M, 2009.

Badger, M. P. S., Schmidt, D. N., Mackensen, A. and Pancost, R. D.: High-resolution alkenone palaeobarometry indicates relatively stable pCO2 during the Pliocene (3.3-2.8 Ma), Philos. T. Roy. Soc. A, 371(2001), 20130094, doi:10.1098/rsta.2013.0094, 2013.

Bartoli, G., Hönisch, B. and Zeebe, R. E.: Atmospheric CO_2 decline during the Pliocene intensification of Northern Hemisphere glaciations, Paleoceanography, 26(4), PA4213, doi:10.1029/2010PA002055, 2011.

Billups K., Ravelo, A. C. and Zachos, J. C.: Early Pliocene deep-water circulation: Stable isotope evidence for enhanced northern component deep water, Proc ODP Sci Results 154, 319–330, 1997.

Briegleb, B. P., Bitz, C. M., Hunke, E. C., Lipscomb, W. H., Holland, M. M., Schramm, J. L., and Moritz, R. E.: Scientific description of the sea ice component in the Community Climate System Model, Version Three., NCAR Technical Note NCAR/TN-463 STR, National Center for Atmospheric Research, Boulder, CO, 2004.

Briegleb, B. P. and Light, B.: A Delta-Eddington Multiple Scattering Parameterization for Solar Radiation in the Sea Ice Component of the Community Climate System Model, NCAR Technical Note NCAR/TN-472+STR 2007, National Center for Atmospheric Research, Boulder, CO, 2007.

Briegleb, B. P., Danabasoglu, G. and Large, W. G.: An Overflow Parametrization for the Ocean Component of the Community Climate System Model, NCAR Technical Note NCAR/TN-481+STR, National Center for Atmospheric Research, Boulder, CO, doi:10.5065/D69K4863, 2010.

Brierley, C. M., Fedorov, A. V., Liu, Z., Herbert, T. D., Lawrence, K. T. and LaRiviere, J. P.: Greatly Expanded Tropical Warm Pool and Weakened Hadley Circulation in the Early Pliocene, Science, 323(5922), 1714–1718, doi:10.1126/science.1167693, 2009.

Brigham-Grette, J., Melles, M., Minyuk, P., Andreev, A., Tarasov, P., DeConto, R. M., Koenig, S. J., Nowaczyk, N., Wennrich, V., Rosén, P., Haltia, E., Cook, T., Gebhardt, C., Meyer-Jacob, C., Snyder, J. and Herzschuh, U.: Pliocene Warmth, Polar Amplification, and Stepped Pleistocene Cooling Recorded in NE Arctic Russia, Science, 340, 1421–1427, 2013.

Cohen, J., Jones, J., Furtado, J. and Tziperman, E.: Warm Arctic, Cold Continents: A Common Pattern Related to Arctic Sea Ice Melt, Snow Advance, and Extreme Winter Weather, oceanog, 26(4), 150–160, doi:10.5670/oceanog.2013.70, 2013.

Collins, William D., Bitz, Cecilia M., Blackmon, Maurice L., Bonan, Gordan B., Bretherton, Christopher S., Carton, James A., Chang, Ping, Doney, Scott C., Hack, James J., Henderson, Thomas B., Kiehl, Jeffrey T., Large, William G., McKenna, Daniel S., Santer, Benjamin D., Smith, Richard D.: The Community Climate System Model Version 3 (CCSM3), J. Climate, 19, 2122–2143, doi:10.1175/JCLI3761.1, 2006.

Collins, M., Knutti, R., Arblaster, J., Dufresne, J.-L., Fichefet, T., Friedlingstein, P., Gao, X., Gutowski, W.J., Johns, T., Krinner, G., Shongwe, M., Tebaldi, C., Weaver, A.J. and Wehner, M.: Long-term Climate Change: Projections, Commitments and Irreversibility. In: Climate Change 2013: The Physical Science Basis. Contribution of Working Group I to the Fifth Assessment Report of the Intergovernmental Panel on Climate Change [Stocker, T.F., Qin, D., Plattner, G.-K., Tignor, M., Allen, S.K., Boschung, J., Nauels, A., Xia, Y., Bex, V. and Midgley, P.M. (eds.)]. Cambridge University Press, Cambridge, United Kingdom and New York, NY, USA, 2013.

Contoux, C., Dumas, C., Ramstein, G., Jost, A. and Dolan, A. M.: Modelling Greenland ice sheet inception and sustainability during the Late Pliocene, Earth and Planetary Science Letters, 424(C), 295–305, doi:10.1016/j.epsl.2015.05.018, 2015.

Cunningham, S. A., Kanzow, T., Rayner, D., Baringer, M. O., Johns, W. E., Marotzke, J., Longworth, H. R., Grant, E. M., Hirschi, J. J. M., Beal, L. M., Meinen, C. S. and Bryden, H. L.: Temporal Variability of the Atlantic Meridional Overturning Circulation at 26.5°N, Science, 317(5840), 935–938, doi:10.1126/science.1141304, 2007.

Danabasoglu, G., Large, W. G. and Briegleb, B. P.: Climate impacts of parameterized Nordic Sea overflows, J. Geophys. Res., 115, C11005, doi:10.1029/2010JC006243, 2010.

Deser, C., Phillips, Adam S., Tomas, Robert A., Okumura, Yuko M., Alexander, Michael A., Capotondi, Antonietta, Scott, James D., Kwon, Young-Oh, and Ohba, Masamichi,: ENSO and Pacific Decadal Variability in the Community Climate System Model Version 4., J. Climate, 25, 2622–2651, doi: 10.1175/JCLI-D-11-00301.1, 2012.

Dowsett, H. J. and Cronin, T. M.: High eustatic sea level during the middle Pliocene: Evidence from the southeastern U.S. Atlantic Coastal Plain, Geology, 18(5), 435–438, doi:10.1130/0091-7613(1990)018<0435:HESLDT>2.3.CO;2, 1990.

Dowsett, H. J., Thompson, R. S., Barron, J. A., Cronin, T. M., Fleming, R. F., Ishman, S.E., Poore, R.Z., Willard, D.A. and Holtz, T.R.: Joint investigations of the middle Pliocene climate I: PRISM paleoenvironmental reconstructions, Global and Planetary Change 9, 169–195, 1994.

Dowsett, H. J., Barron, J. A., Poore, R. Z., Thompson, R. S., Cronin, T. M., Ishman, S. E., and Willard, D. A.: Middle Pliocene paleoenvironmental reconstruction—PRISM2, U.S. Geological Survey Open-File Report 99–535, 1 v.(unpaged), maps, 1999.

Dowsett, H. J., Robinson, M. M., Stoll, D. K. and Foley, K. M.: Mid-Piacenzian mean annual sea surface temperature analysis for data-model comparisons, Stratigraphy, 7(2-3), 189–198, 2010.

Dowsett, H. J., Robinson, M. M., Haywood, A. M., Hill, D. J., Dolan, A. M., Stoll, D. K., Chan, W.-L., Abe-Ouchi, A., Chandler, M. A., Rosenbloom, N. A., Otto-Bliesner, B. L., Bragg, F. J., Lunt, D. J., Foley, K. M. and Riesselman, C. R.: Assessing confidence in Pliocene sea surface temperatures to evaluate predictive models, Nature Climate Change, 2(5), 365–371, doi:10.1038/nclimate1455, 2012.

Dowsett, H. J., Foley, K. M., Stoll, D. K., Chandler, M. A., Sohl, L. E., Bentsen, M., Otto-Bliesner, B. L., Bragg, F. J., Chan, W.-L., Contoux, C., Dolan, A. M., Haywood, A. M., Jonas, J. A., Jost, A., Kamae, Y., Lohmann, G., Lunt, D. J., Nisancioglu, K. H., Ramstein, G., Abe-Ouchi, A., Riesselman, C. R., Robinson, M. M., Rosenbloom, N. A., Salzmann, U., Stepanek, C., Strother, S. L., Ueda, H., Yan, Q. and Zhang, Z.: Sea Surface Temperature of the mid-Piacenzian Ocean: A Data-Model Comparison, Sci. Rep., 3(2013), doi:10.1038/srep02013, 2013.

Dowsett, H., Dolan, A., Rowley, D., Moucha, R., Forte, A. M., Mitrovica, J. X., Pound, M., Salzmann, U., Robinson, M., Chandler, M., Foley, K. and Haywood, A.: The PRISM4 (mid-Piacenzian) paleoenvironmental reconstruction, Clim. Past, 12(7), 1519–1538, doi:10.5194/cp-12-1519-2016, 2016.

Dwyer, G. S. and Chandler, M. A.: Mid-Pliocene sea level and continental ice volume based on coupled benthic Mg/Ca palaeotemperatures and oxygen isotopes, Philos. T. Roy. Soc. A, 367(1886), 157–168, doi:10.1098/rsta.2008.0222, 2009.

Fedorov, A. V., Brierley, C. M., Lawrence, K. T., Liu, Z., Dekens, P. S. and Ravelo, A. C.: Patterns and mechanisms of early Pliocene warmth, Nature, 496(7443), 43–49, doi:10.1038/nature12003, 2013.

Frank, M., Whiteley, N., Kasten, S., Hein, J. R. and O'Nions, K.: North Atlantic Deep Water export to the Southern Ocean over the past 14 Myr: Evidence from Nd and Pb isotopes in ferromanganese crusts, Paleoceanography, 17(2), 1022, doi:10.1029/2000PA000606, 2002.

Frenz, M., Henrich, R. and Zychla, B.: Carbonate preservation patterns at the Ceará Rise – Evidence for the Pliocene super conveyor, Marine Geology, 232(3-4), 173–180, doi:10.1016/j.margeo.2006.07.006, 2006.

Gent, P. R., Danabasoglu, G., Donner, L. J., Holland, M. M., Hunke, E. C., Jayne, S. R., Lawrence, D. M., Neale, R. B., Rasch, P. J., Vertenstein, M., Worley, P. H., Yang, Z.-L., and Zhang, M.: The Community Climate System Model Version 4, J. Climate, 24, 4973–4991, doi:10.1175/2011JCLI4083.1, 2011.

Fretwell, P., Pritchard, H. D., Vaughan, D. G., Bamber, J. L., Barrand, N. E., Bell, R. E., Bianchi, C., Bingham, R. G., Blankenship, D. D., Casassa, G., Catania, G., Callens, D., Conway, H., Cook, A. J., Corr, H. F. J., Damaske, D., Damm, V., Ferraccioli, F., Forsberg, R., Fujita, S., Gim, Y., Gogineni, P., Griggs, J. A., Hindmarsh, R. C. A., Holmlund, P., Holt, J. W., Jacobel, R. W., Jenkins, A., Jokat, W., Jordan, T., King, E. C., Kohler, J., Krabill, W. B., Riger-Kusk, M., Langley, K. A., Leitchenkov, G., Leuschen, C., Luyendyk, B. P., Matsuoka, K., Mouginot, J., Nitsche, F. O., Nogi, Y., Nost, O. A., Popov, S. V., Rignot, E., Rippin, D. M., Rivera, A., Roberts, J., Ross, N., Siegert, M. J., Smith, A. M., Steinhage, D., Sun, B., Tinto, B. K., Welch, B. C., Wilson, D., Young, D. A., Xiangbin, C. and Zirizzotti, A.: Bedmap2: improved ice bed, surface and thickness datasets for Antarctica, The Cryosphere, 7(1), 375–393, doi:10.5194/tc-7-375-2013, 2013.

Haywood, A. M. and Valdes, P. J.: Modelling Pliocene warmth: contribution of atmosphere, oceans and cryosphere, Earth and Planetary Science Letters, 218, 363–377, doi:10.1016/S0012-821X(03)00685-X, 2004.

Haywood, A. M., Hill, D. J., Dolan, A. M., Otto-Bliesner, B. L., Bragg, F. J., Chan, W.-L., Chandler, M. A., Contoux, C., Dowsett, H. J., Jost, A., Kamae, Y., Lohmann, G., Lunt, D. J., Abe-Ouchi, A., Pickering, S. J., Ramstein, G., Rosenbloom, N. A., Salzmann, U., Sohl, L. E., Stepanek, C., Ueda, H., Yan, Q. and Zhang, Z.: Large-scale features of Pliocene climate: results from the Pliocene Model Intercomparison Project, Clim. Past, 9(1), 191–209, doi:10.5194/cp-9-191-2013, 2013.

Haywood, A. M., Dowsett, H. J., Dolan, A. M., Rowley, D., Abe-Ouchi, A., Otto-Bliesner, B. L., Chandler, M. A., Hunter, S. J., Lunt, D. J., Pound, M. and Salzmann, U.: The Pliocene Model Intercomparison Project (PlioMIP) Phase 2: scientific objectives and experimental design, Clim. Past, 12(3), 663–675, doi:10.5194/cp-12-663-2016, 2016.

Holland, M. M., Bailey, D. A., Briegleb, B. P., Light, B. and Hunke, E. C.: Improved Sea Ice Shortwave Radiation Physics in CCSM4: The Impact of Melt Ponds and Aerosols on Arctic Sea Ice*, J. Climate, 25(5), 1413–1430, doi:10.1175/JCLI-D-11-00078.1, 2012.

Hu, A., Meehl, G. A., Han, W., Otto-Bliestner, B., Abe-Ouchi, A. and Rosenbloom, N.: Effects of the Bering Strait closure on AMOC and global climate under different background climates, Progress in Oceanography, 132(C), 174–196, doi:10.1016/j.pocean.2014.02.004, 2015.

Hunke, E. and Lipscomb, W. H.: CICE: The Los Alamos sea ice model, documentation and software, version 4.0, Los Alamos National Laboratory Tech. Rep. LA-CC-06-012, 76 pp., 2008.

Kamae, Y., Yoshida, K. and Ueda, H.: Sensitivity of Pliocene climate simulations in MRI-CGCM2.3 to respective boundary conditions, Clim. Past, 12, 1619–1634, doi:10.5194/cp-12-1619-2016, 2016.

Kennett, J. P. and Hodell, D. A.: Evidence for Relative Climatic Stability of Antarctica during the Early Pliocene: A Marine Perspective, Geogr. Ann., 75(4), 205–220, 1993.

Kennett, J. P. and Hodell, D. A.: Stability or instability of Antarctic ice sheets during warm climates of the Pliocene?, GSA Today, 5(1), 10–13, 1995.

Kürschner, W. M., van der Burgh, J., Visscher, H. and Dilcher, D. L.: Oak leaves as biosensors of late Neogene and early Pleistocene paleoatmospheric CO2 concentrations, Mar. Micropaleontol., 27, 299–312, 1996.

Krantz, D. E.: A Chronology of Pliocene Sea-Level Fluctutations: the U.S. Middle Atlantic Coastal Plain Record, Quaternary Sci. Rev., 10, 163–174, 1991.

Large, W. G., and Danabasoglu, G.: Attribution and impacts of upper-ocean biases in CCSM3. J. Climate, 19, 2335–2346, 2006.

Lawrence, P. J. and Chase, T. N.: Representing a new MODIS consistent land surface in the Community Land Model (CLM3.0), J. Geophys. Res., 112, G01023, doi:10.1029/2006JG000168, 2007.

Lawrence, D. M., Oleson, K. W., Flanner, M. G., Fletcher, C. G., Lawrence, P. J., Levis, S., Swenson, S. C., and Bonan, G. B.: The CCSM4 Land Simulation, 1850–2005: Assessment of Surface Climate and New Capabilities, J. Climate, 25, 2240–2260, doi:10.1175/JCLI-D-11-00103.1, 2012.

Lawrence, K. T., Herbert, T. D., Brown, C. M., Raymo, M. E. and Haywood, A. M.: High-amplitude variations in North Atlantic sea surface temperature during the early Pliocene warm period, Paleoceanography, 24(2), PA2218, doi:10.1029/2008PA001669, 2009.

Levitus, S. and Boyer, T. P.: World Ocean Atlas, Volume 4: Temperature NOAA Atlas NESDIS 4, U.S. Government Printing Office, 1994.

Lunt, D. J., Foster, G. L., Haywood, A. M. and Stone, E. J.: Late Pliocene Greenland glaciation controlled by a decline in atmospheric CO2 levels, Nature, 454(7208), 1102–1105, doi:10.1038/nature07223, 2008.

Lunt, D. J., Haywood, A. M., Schmidt, G. A., Salzmann, U., Valdes, P. J., Dowsett, H. J. and Loptson, C. A.: On the causes of mid-Pliocene warmth and polar amplification, Earth and Planetary Science Letters, 321-322(C), 128–138, doi:10.1016/j.epsl.2011.12.042, 2012.

Martínez-Botí, M. A., Foster, G. L., Chalk, T. B., Rohling, E. J., Sexton, P. F., Lunt, D. J., Pancost, R. D., Badger, M. P. S. and Schmidt, D. N.: Plio-Pleistocene climate sensitivity evaluated using high-resolution CO2 records, Nature, 518(7537), 49–54, doi:10.1038/nature14145, 2015.

McCarthy, G., Smeed, D., Johns, W., Frajka-Williams, E., Moat, B., Rayner, D., Baringer, M., Meinen, C., Collins, J., and Bryden, H.: Measuring the Atlantic meridional overturning circulation at 26°N, Prog. Oceanogr., 130, 91–111, 2015

McKay, R., Naish, T. R., Carter, L., Riesselman, C. R., Dunbar, R. B., Sjunneskog, C., Winter, D., Sangiorgi, F., Warren, C., Pagani, M., Schouten, S., Willmott, V., Levy, R., DeConto, R. M. and Powell, R.: Antarctic and Southern Ocean influences on Late Pliocene global cooling, PNAS, 109(17), 6423–6428, doi:10.1073/pnas.1112248109/, 2012.

Miller, K. G., Wright, J. D., Browning, J. V., Kulpecz, A., Kominz, M. A., Naish, T. R., Cramer, B. S., Rosenthal, Y., Peltier, W. R. and Sosdian, S.: High tide of the warm Pliocene: Implications of global sea level for Antarctic deglaciation, Geology, 40(5), 407–410, doi:10.1130/G32869.1, 2012.

Moucha, R., Mitrovica, J. X., Forte, A. M., Rowley, D. B., Quéré, S., Simmons, N. A. and Grand, S. P.: Dynamic topography and long-term sea-level variations: There is no such thing as a stable continental platform, Earth and Planetary Science Letters, 271(1-4), 101–108, doi:10.1016/j.epsl.2008.03.056, 2008.

Naish, T. R. and Wilson, G. S.: Constraints on the amplitude of Mid-Pliocene (3.6-2.4Ma) eustatic sea-level fluctuations from the New Zealand shallow-marine sediment record, Philos. T. Roy. Soc. A, 367(1886), 169–187, doi:10.1098/rsta.2008.0223, 2009.

Neale, R. B., Richter, J., Park, S., Lauritzen, P. H., Vavrus, S. J., Rasch, P. J., and Zhang, M.: The Mean Climate of the Community Atmosphere Model (CAM4) in Forced SST and Fully Coupled Experiments, J. Climate, 26, doi:10.1175/JCLI-D-12-00236.1, 2013.

O'Brien, C. L., Foster, G. L., Martínez-Botí, M. A., Abell, R., Rae, J. W. B. and Pancost, R. D.: High sea surface temperatures in tropical warm pools during the Pliocene, Nature Geosci, 7(8), 606–611, doi:10.1038/ngeo2194, 2014.

Overland, J. E., Wood, K. R. and Wang, M.: Warm Arctic—cold continents: climate impacts of the newly open Arctic Sea, Polar Research, 30(0), 4045–14, doi:10.3402/polar.v30i0.15787, 2011.

Pagani, M., Liu, Z., LaRiviere, J. P. and Ravelo, A. C.: High Earth-system climate sensitivity determined from Pliocene carbon dioxide concentrations, Nature Geosci, 3(1), 27–30, doi:10.1038/ngeo724, 2010.

Peltier, W. R. and Vettoretti, G.: Dansgaard-Oeschger oscillations predicted in a comprehensive model of glacial climate: A "kicked" salt oscillator in the Atlantic, Geophys. Res. Lett., 41(20), 7306–7313, doi:10.1002/2014GL061413, 2014.

Prentice, I. C., Cramer, W., Harrison, S. P., Leemans, R., Monserud, R. A., and Solomon, A. M.: A global biome model based on plant physiology and dominance, soil properties and climate, J. Biogeogr., 19, 117–134, 1992

Ravelo, A. C. and Andreasen, D. H.: Enhanced circulation during a warm period, Geophys. Res. Lett., 27(7), 1001–1004, doi:10.1029/1999GL007000, 2000.

Raymo, M. E., Grant, B., Horowitz, M. and Rau, G. H.: Mid-Pliocene warmth: stronger greenhouse and stronger conveyor, Mar. Micropaleontol., 27, 313–326, 1996.

Robinson, M. M., Dowsett, H. J., Dwyer, G. S. and Lawrence, K. T.: Reevaluation of mid-Pliocene North Atlantic sea surface temperatures, Paleoceanography, 23, PA3213, doi:10.1029/2008PA001608, 2008.

Rosenbloom, N. A., Otto-Bliesner, B. L., Brady, E. C. and Lawrence, P. J.: Simulating the mid-Pliocene Warm Period with the CCSM4 model, Geosci. Model Dev., 6(2), 549–561, doi:10.5194/gmd-6-549-2013, 2013.

Rowley, D. B., Forte, A. M., Moucha, R., Mitrovica, J. X., Simmons, N. A. and Grand, S. P.: Dynamic Topography Change of the Eastern United States Since 3 Million Years Ago, Science, 340(6140), 1560–1563, doi:10.1126/science.1229180, 2013.

Rybczynski, N., Gosse, J. C., Harington, C. R., Wogelius, R. A., Hidy, A. J. and Buckley, M.: Mid-Pliocene warm-period deposits in the High Arctic yield insight into camel evolution, Nature Communications, 4, 1550, doi:10.1038/ncomms2516, 2013.

Salzmann, U., Haywood, A. M., Lunt, D. J., Valdes, P. J. and Hill, D. J.: A new global biome reconstruction and data-model comparison for the Middle Pliocene, Global Ecology and Biogeography, 17(3), 432–447, doi:10.1111/j.1466-8238.2008.00381.x, 2008.

Seki, O., Foster, G. L., Schmidt, D. N., Mackensen, A., Kawamura, K. and Pancost, R. D.: Alkenone and boron-based Pliocene pCO2 records, Earth and Planetary Science Letters, 292(1-2), 201–211, doi:10.1016/j.epsl.2010.01.037, 2010.

Sohl, L. E., Chandler, M. A., Schmunk, R. B., Mankoff, K., Jonas, J. A., Foley, K. M. and Dowsett, H. J.: PRISM3/GISS Topographic Reconstruction. 2009.

Smith, R., Jones, P., Briegleb, B., Bryan, F., Danabasoglu, G., Dennis, J., Dukowicz, J., Eden, C., Fox-Kemper, B., Gent, P., Hecht, M., Jayne, S., Jochum, M., Large, W., Lindsay, K., Maltrud, M., Norton, N., Peacock, S., Vertenstein, M., and Yeager, S.: The Parallel Ocean Program (POP) reference manual, ocean component of the Community Climate System Model (CCSM), Los Alamos National Laboratory Tech. Rep. LAUR-10-01853, 141 pp., 2010.

Subramanian, A. C., Jochum, M., Miller, A. J., Murtugudde, R., Neale, R. B. and Waliser, D. E.: The Madden-Julian Oscillation in CCSM4, J. Climate, 24(24), 6261–6282, doi:10.1175/JCLI-D-11-00031.1, 2011.

Sun, L., Perlwitz, J. and Hoerling, M.: What caused the recent "Warm Arctic, Cold Continents" trend pattern in winter temperatures? Geophys. Res. Lett., 43(10), 5345–5352, doi:10.1002/2016GL069024, 2016.

Trenberth, K. E. and Caron, J. M.: Estimates of Meridional Atmosphere and Ocean Heat Transport, J. Climate, 14, 3433–3443, 2001.

Tripati, A. K., Roberts, C. D. and Eagle, R. A.: Coupling of CO2 and Ice Sheet Stability Over Major Climate Transitions of the Last 20 Million Years, Science, 326(5958), 1394–1397, doi:10.1126/science.1178296, 2009.

Vettoretti, G. and Peltier, W. R.: Last Glacial Maximum ice sheet impacts on North Atlantic climate variability: The importance of the sea ice lid, Geophys. Res. Lett., 40(24), 6378–6383, doi:10.1002/2013GL058486, 2013.

Wardlaw, B. R. and Quinn, T. M.: The Record of Pliocene Sea-Level Change at Enewetak Atoll, Quaternary Sci. Rev., 10, 247–258, 1991.

Weertman, J.: Stability of the junction of an ice sheet and an ice shelf, Journal of Glaciology, 13(67), 3–11, 1974.

Winnick, M. J. and Caves, J. K.: Oxygen isotope mass-balance constraints on Pliocene sea level and East Antarctic Ice Sheet stability, Geology, 43(10), 879–882, doi:10.1130/G36999.1, 2015.

Zhang, Y. G., Pagani, M., Liu, Z., Bohaty, S. M. and DeConto, R. M.: A 40-million-year history of atmospheric CO_2 , Philos. T. Roy. Soc. A, 371(2001), 20130096, doi:10.1098/rsta.2013.0096, 2013a.

Zhang, Z. S., Nisancioglu, K. H., Chandler, M. A., Haywood, A. M., Otto-Bliesner, B. L., Ramstein, G., Stepanek, C., Abe-Ouchi, A., Chan, W.-L., Bragg, F. J., Contoux, C., Dolan, A. M., Hill, D. J., Jost, A., Kamae, Y., Lohmann, G., Lunt, D. J., Rosenbloom, N. A., Sohl, L. E. and Ueda, H.: Mid-pliocene Atlantic Meridional Overturning Circulation not unlike modern, Clim. Past, 9(4), 1495–1504, doi:10.5194/cp-9-1495-2013, 2013b.

Clim. Past Discuss., doi:10.5194/cp-2017-21, 2017
Manuscript under review for journal Clim. Past
Discussion started: 24 February 2017

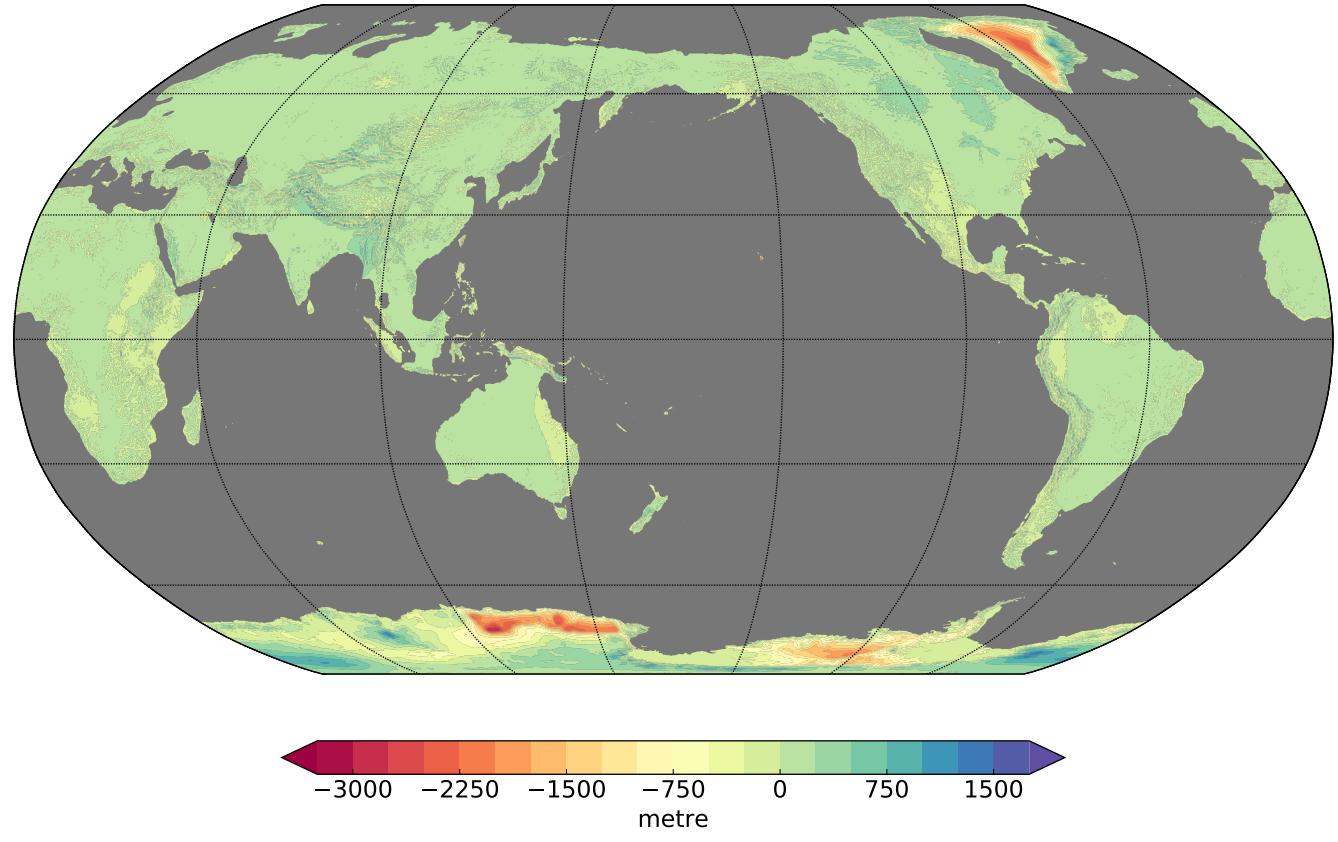

Figure 1. The topography anomaly field which when superimposed on our local modern day topography results in the PRISM4 mid-Pliocene topography.

Clim. Past Discuss., doi:10.5194/cp-2017-21, 2017
Manuscript under review for journal Clim. Past
Discussion started: 24 February 2017

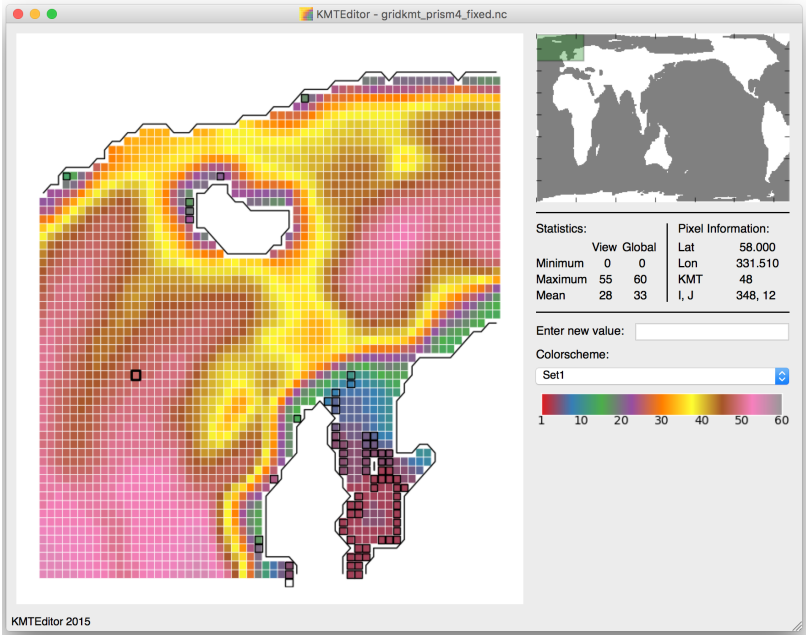

Figure 2. A screenshot of one of our graphical tools for editing the ocean model's grid. The dark black square in the left side plot is the cursor which can be used to navigate over to individual cells in order to change their values. The cells which are outlined by a thin dark border denote those cells whose values have been edited.

Clim. Past Discuss., doi:10.5194/cp-2017-21, 2017
Manuscript under review for journal Clim. Past
Discussion started: 24 February 2017

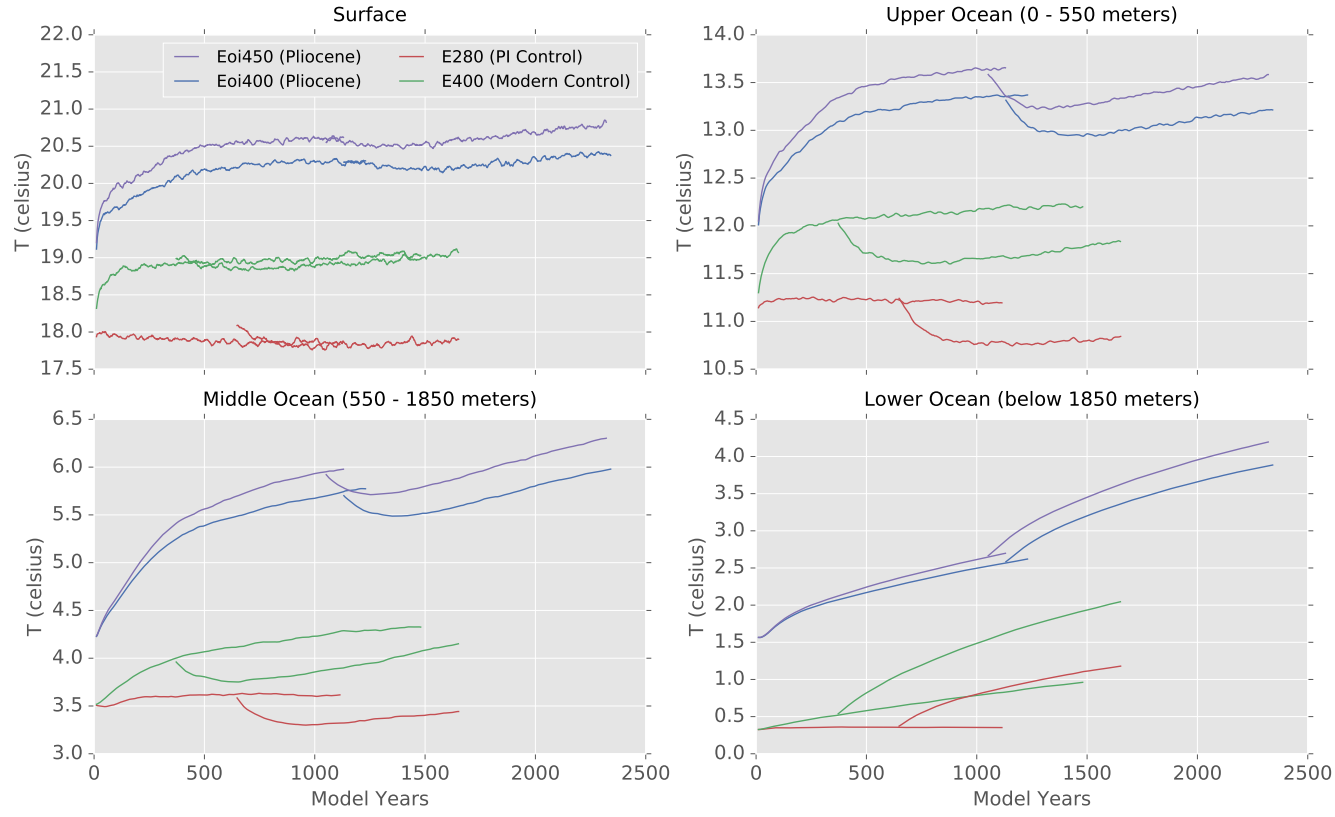

Figure 3. Evolution of the ocean temperature at different depths. When a new curve "forks" from an existing curve it represents the branching of the P version of that simulation in which the ocean model's κ has been fixed to the POP1 type profile. In all cases the original simulation (with $\kappa = 0.16$ throughout the ocean) was also continued further for some more time. (a) the evolution of the sea surface temperature, (b), (c) and (d) are the volume averaged temperatures in the upper ocean (0-550 meters), middle ocean (550-1850 meters) and lower ocean (below 1850 meters) respectively.

Clim. Past Discuss., doi:10.5194/cp-2017-21, 2017
Manuscript under review for journal Clim. Past
Discussion started: 24 February 2017

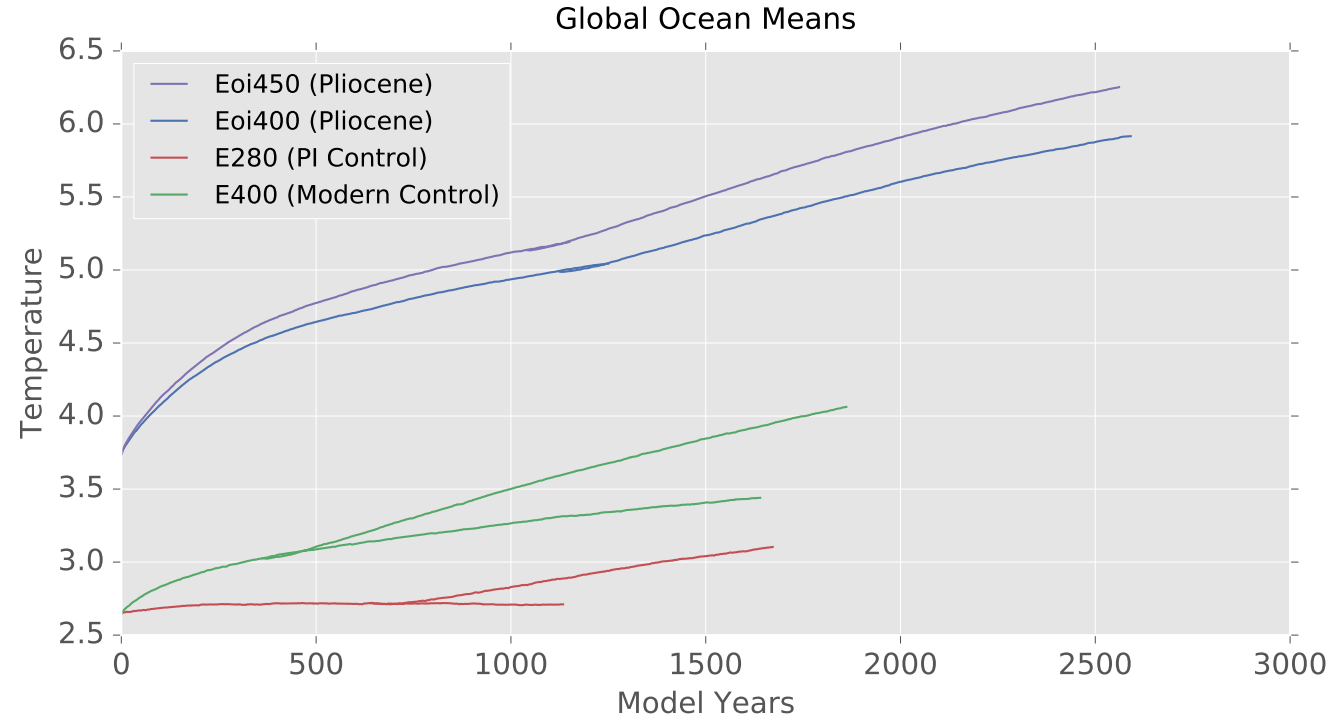

Figure 4. Similar to Figure 3 but instead showing the evolution of the globally averaged ocean temperature.

Clim. Past Discuss., doi:10.5194/cp-2017-21, 2017
Manuscript under review for journal Clim. Past
Discussion started: 24 February 2017

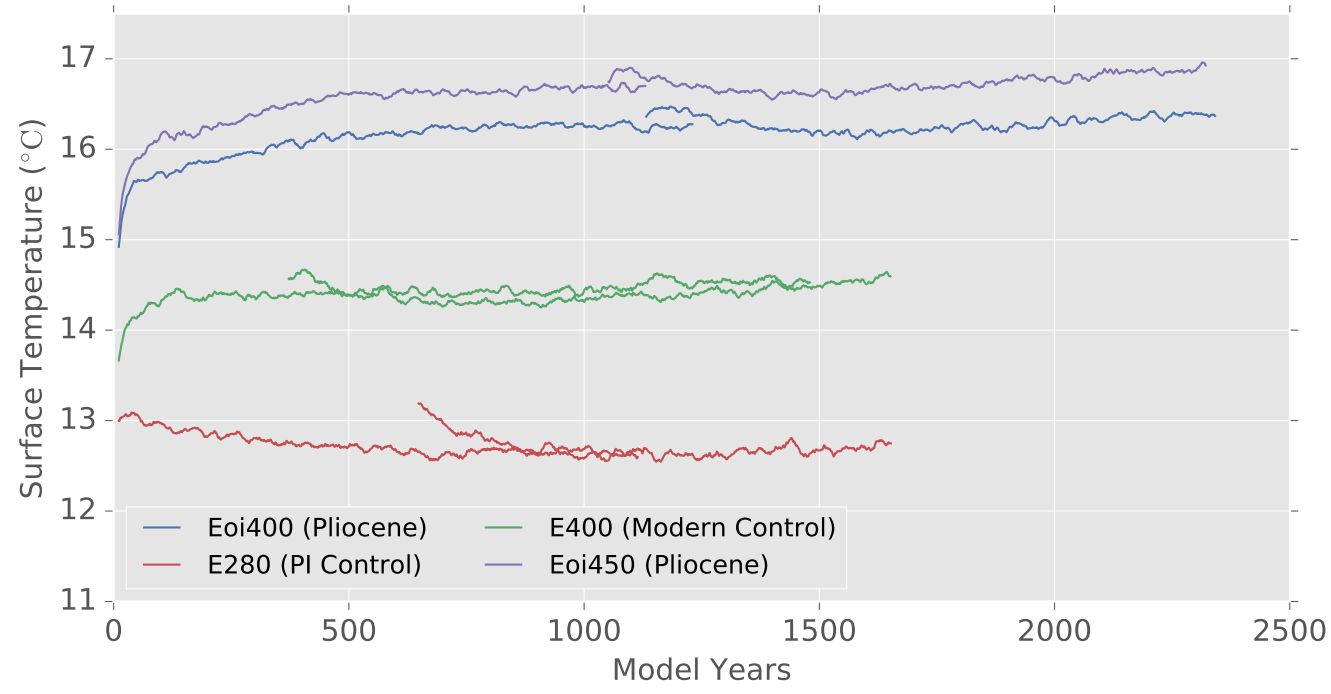

Figure 5. Evolution of the surface air temperatures. When a new curve "forks" from an existing curve it represents the branching of the P version of that simulation in which the ocean model's κ has been fixed to the POP1 type profile. In all cases the original simulation (with $\kappa = 0.16$ throughout the ocean) was also continued further for some more time.

Clim. Past Discuss., doi:10.5194/cp-2017-21, 2017
Manuscript under review for journal Clim. Past
Discussion started: 24 February 2017

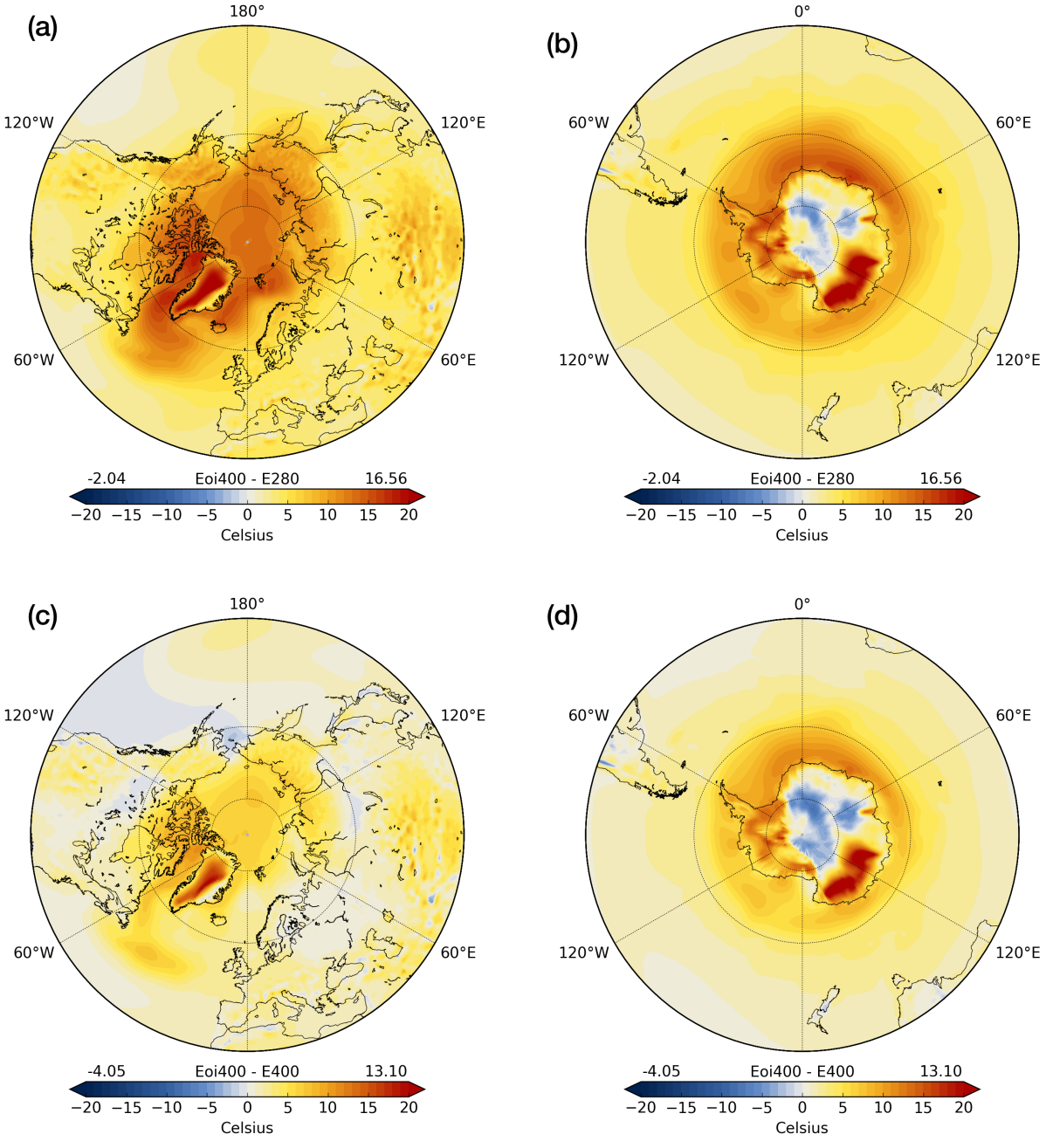

Figure 6. Surface air temperature anomalies for the $\mathrm{E}oi^{400}{}_{\mathrm{P}}$ mid-Pliocene simulation compared to the pre-industrial control $\mathrm{E}^{280}{}_{\mathrm{P}}$ (a) and (b), and compared to the modern control $\mathrm{E}^{400}{}_{\mathrm{P}}$ (c) and (d).

Clim. Past Discuss., doi:10.5194/cp-2017-21, 2017
Manuscript under review for journal Clim. Past
Discussion started: 24 February 2017

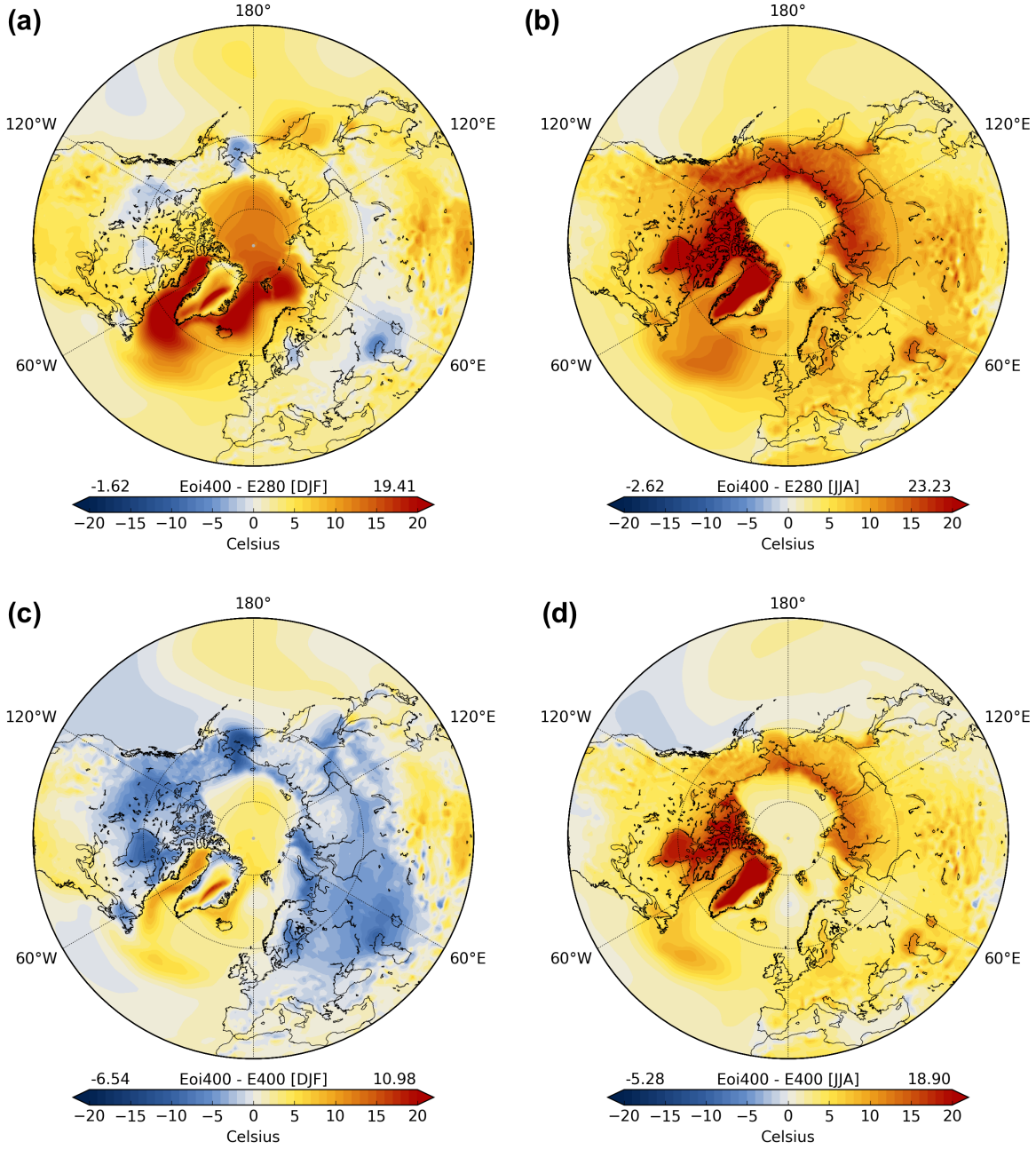

Figure 7. Similar to Figure 6 but instead showing the mean seasonal surface temperature anomalies. (a) and (c) are for DJF, (b) and (d) are for JJA.

Clim. Past Discuss., doi:10.5194/cp-2017-21, 2017
Manuscript under review for journal Clim. Past
Discussion started: 24 February 2017

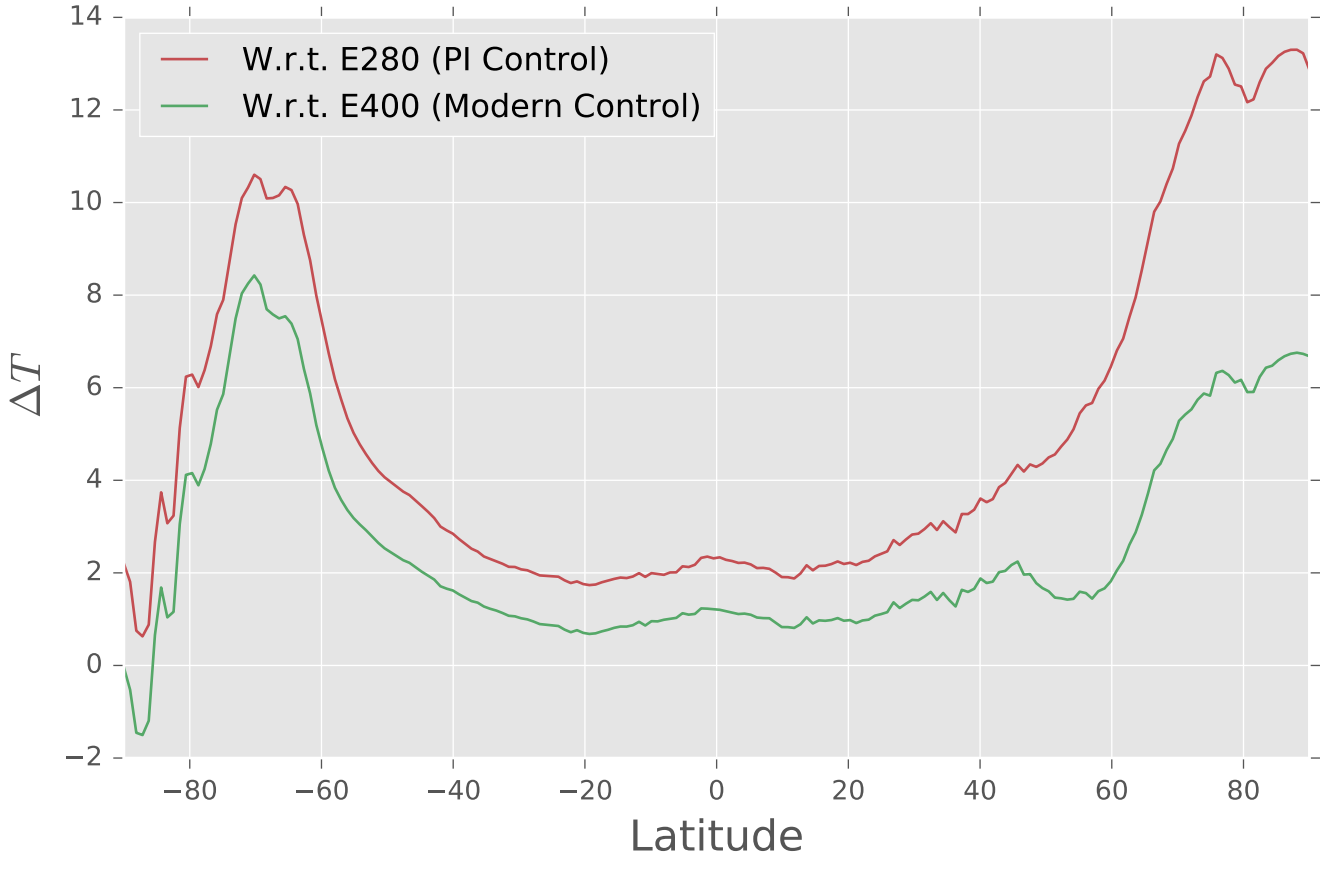

Figure 8. The zonally averaged surface air temperature anomalies for the $Eoi^{400}{}_{\mathrm{P}}$ mid-Pliocene simulation compared to the PI control and the modern control.

Clim. Past Discuss., doi:10.5194/cp-2017-21, 2017
Manuscript under review for journal Clim. Past
Discussion started: 24 February 2017

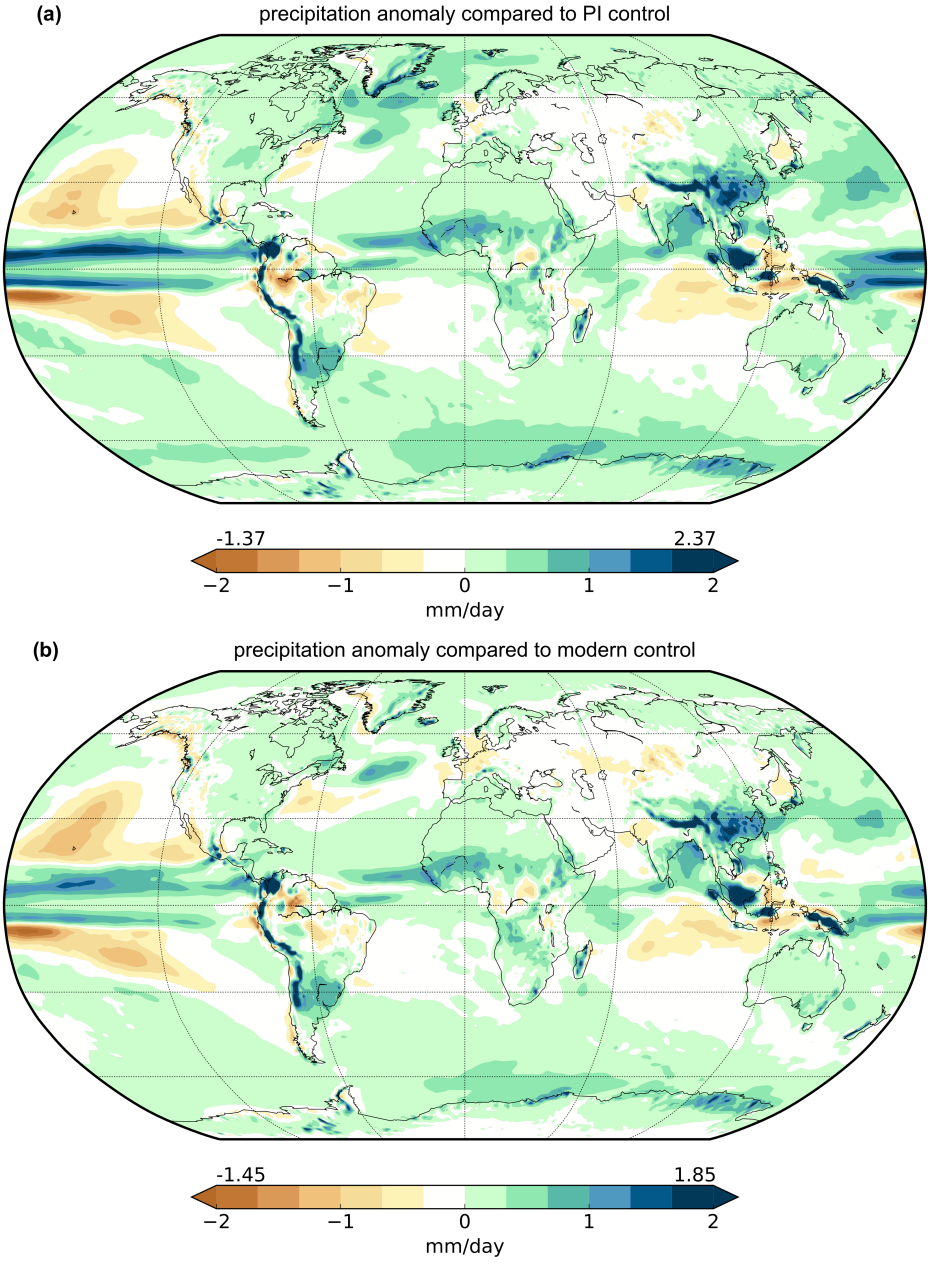

Figure 9. The annual precipitation anomaly between the Eoi^{400}P mid-Pliocene simulation and (a) the PI control and, (b) the modern control. Anomaly is defined as Pliocene - control.

Clim. Past Discuss., doi:10.5194/cp-2017-21, 2017
Manuscript under review for journal Clim. Past
Discussion started: 24 February 2017

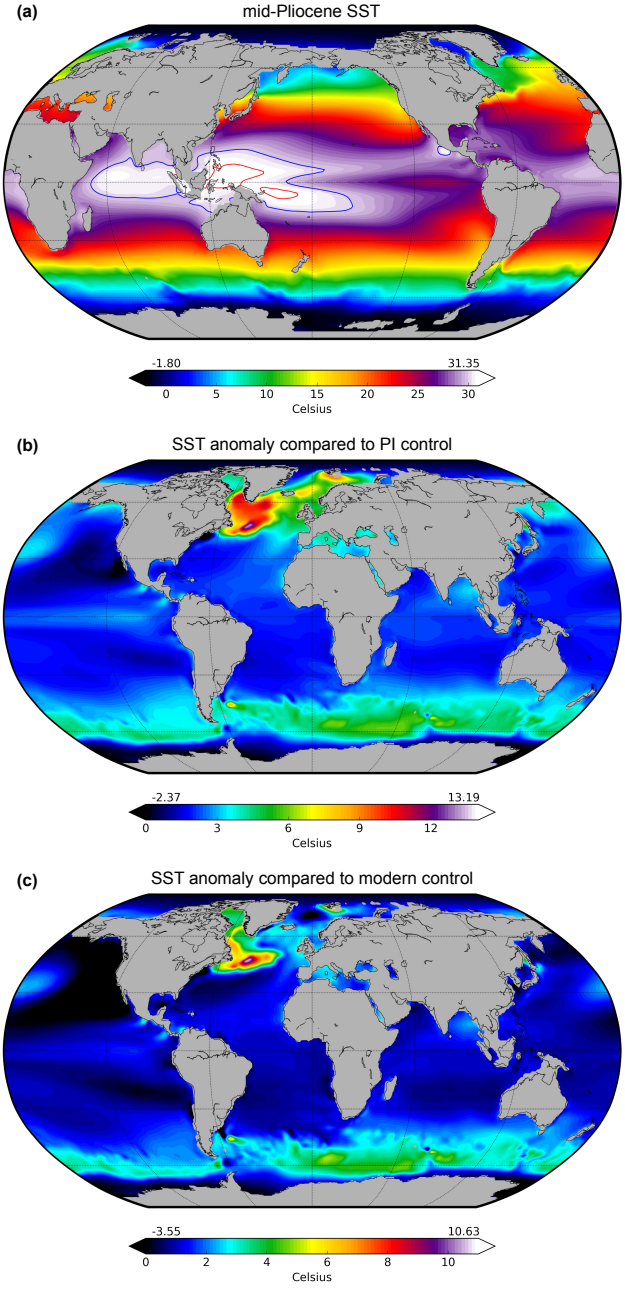

Figure 10. (a) The mid-Pliocene SST from the Eoi^{400}P simulation. The blue and the red contours are for 30°C and 31°C temperatures respectively. The SST anomaly with (b) PI control and, (c) modern control. Anomaly is defined as Pliocene - control.

Clim. Past Discuss., doi:10.5194/cp-2017-21, 2017
Manuscript under review for journal Clim. Past
Discussion started: 24 February 2017

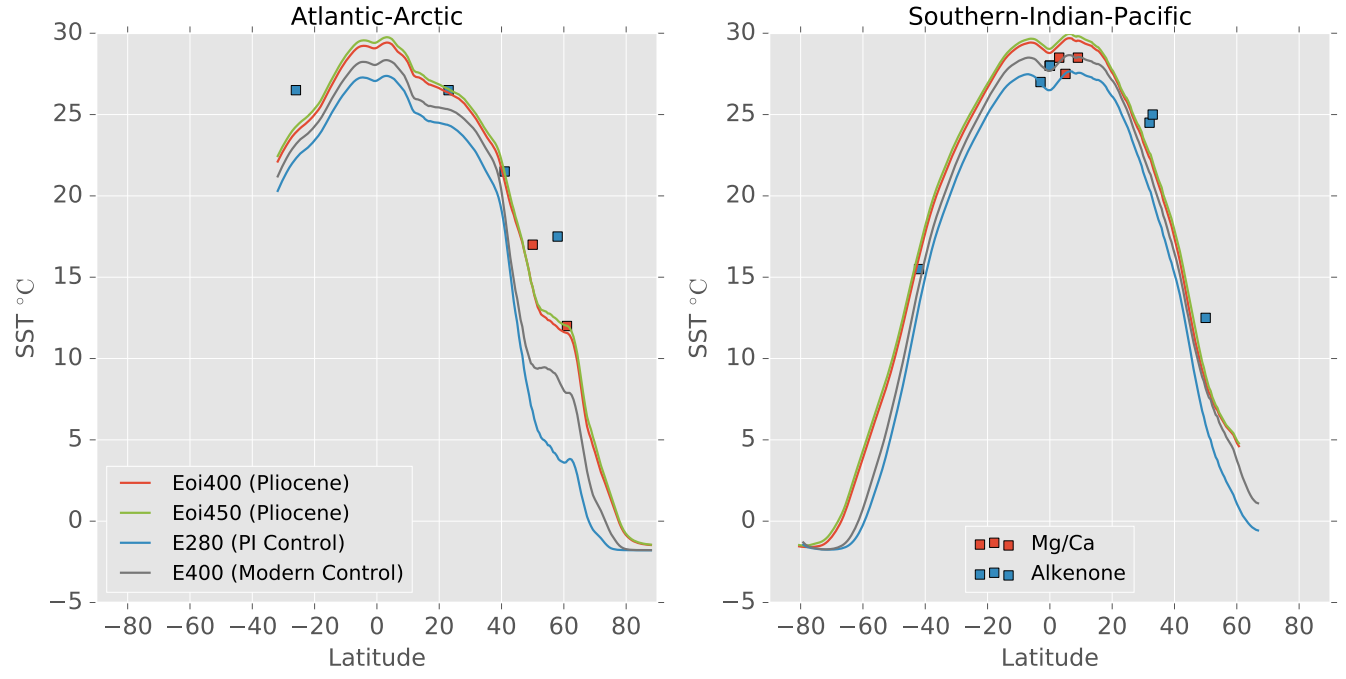

Figure 11. The zonal-mean SST for two oceanic basins computed as a function of latitude. On the left is the zonal means over the Atlantic and the Arctic basins, and the zonal mean over the Southern, Indian and the Pacific Ocean is shown on the right. The black markers are data points (compilation by *Brierley et al.* (2009)) representing proxy inferred mid-Pliocene SSTs.

Clim. Past Discuss., doi:10.5194/cp-2017-21, 2017
Manuscript under review for journal Clim. Past
Discussion started: 24 February 2017

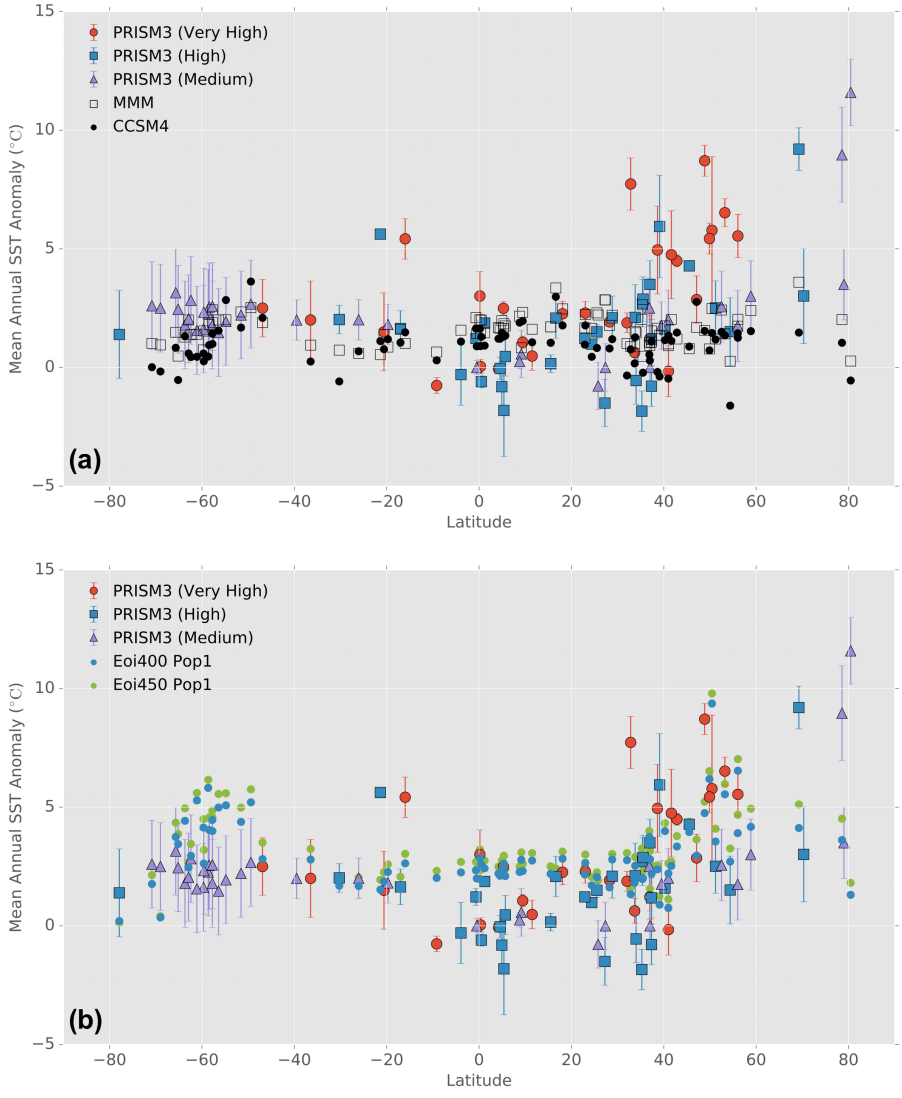

Figure 12. Data-model comparison of the mid-Pliocene SST anomaly compared to pre-industrial. The data in both (a) and (b) are the PRISM3 estimates (*Dowsett et al.*, 2010) which have been categorized into three confidence categories (*Dowsett et al.*, 2012). (a) compares the PRISM3 estimates to the multi-model mean from PlioMIP1 (transparent black square markers), and to the anomalies obtained by *Rosenbloom et al.* (2013) for PlioMIP1 (black dots) using the same CCSM4 model that we are using in this study. (b) compares the PRISM3 estimates to the anomalies obtained from our two mid-Pliocene simulations $Eoi^{400}{}_{\mathrm{P}}$ and $Eoi^{450}{}_{\mathrm{P}}$, shown in blue and green dots respectively.

Clim. Past Discuss., doi:10.5194/cp-2017-21, 2017
Manuscript under review for journal Clim. Past
Discussion started: 24 February 2017

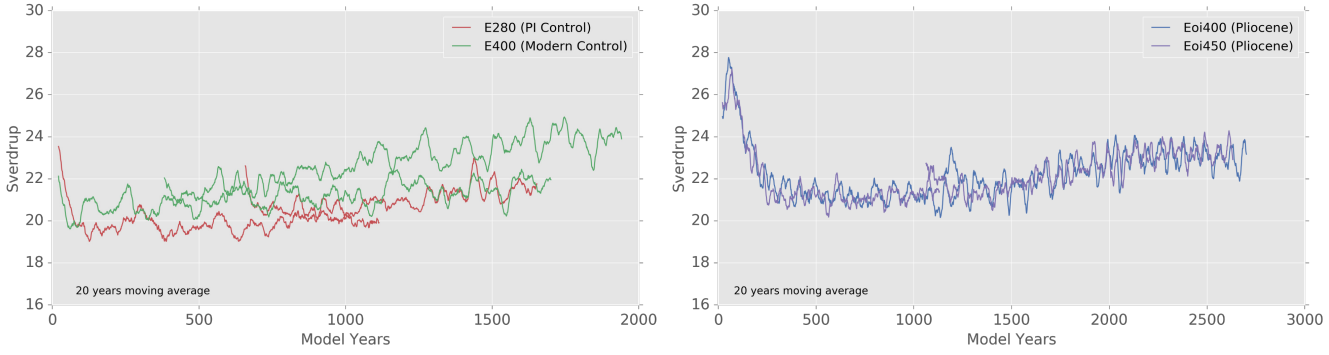

Figure 13. Evolution of the maximum of the Atlantic Meridional Overturning Circulation. The results shown have been filtered with a 20 year running mean to remove high-frequency variability. For each simulation the curve that starts at model year zero is for the version that uses a vertically constant background diapycnal diffusivity while the curve with identical color that starts mid-way is for the version which uses the CCSM3/POP1 type vertical profile of diapycnal diffusivity.

Clim. Past Discuss., doi:10.5194/cp-2017-21, 2017
Manuscript under review for journal Clim. Past
Discussion started: 24 February 2017

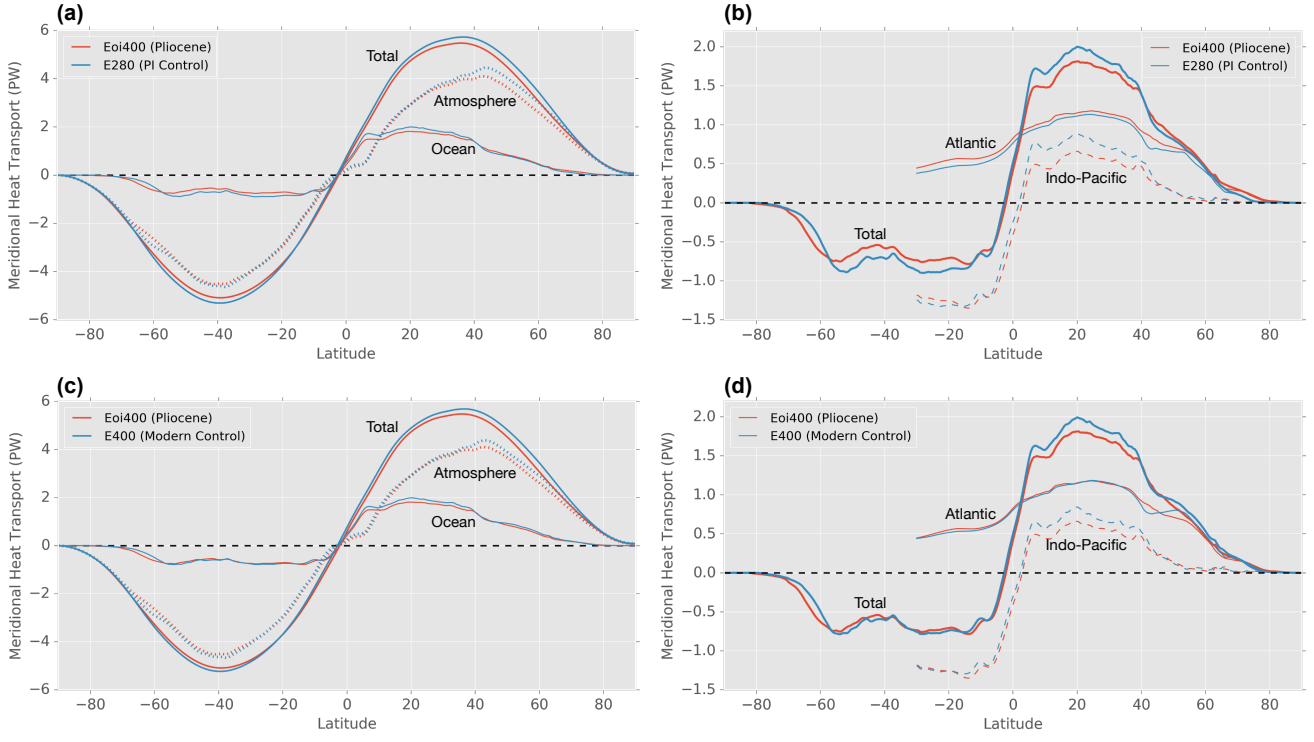

Figure 14. Total meridional heat transport and its decomposition. The top (bottom) row compares the Eoi^{400}P mid-Pliocene simulation to the PI (modern) control. The left column shows the total meridional heat transport and its decomposition into the atmospheric and oceanic components. The right column decomposes the oceanic components into the transport in the Atlantic and the Indo-Pacific basins.

Clim. Past Discuss., doi:10.5194/cp-2017-21, 2017
Manuscript under review for journal Clim. Past
Discussion started: 24 February 2017

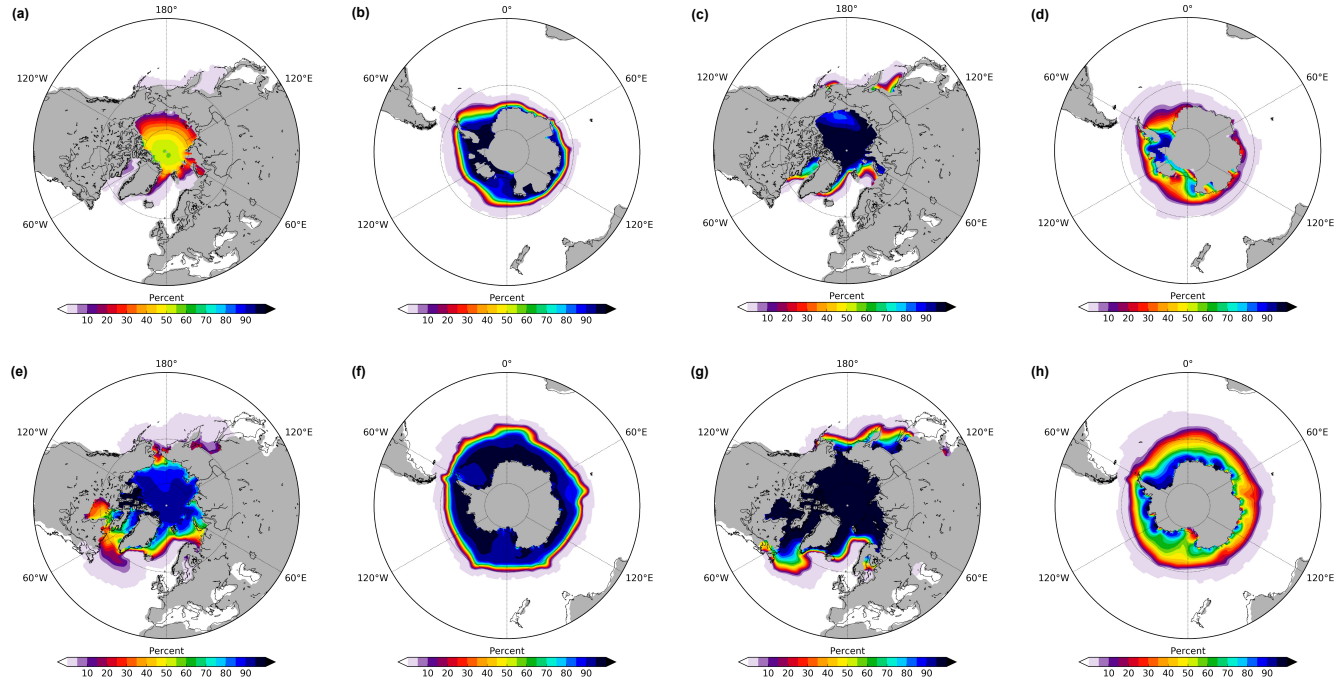

Figure 15. Surface area covered by sea ice for the mid-Pliocene (a)-(d) and PI control (e)-(h). The climatological mean for the austral winter months JJA is presented in the first two columns, and the boreal winter months DJF in the last two columns.

Clim. Past Discuss., doi:10.5194/cp-2017-21, 2017
Manuscript under review for journal Clim. Past
Discussion started: 24 February 2017

Climate of the Past Discussions
Open Access
EGU

Table 1. Configuration common to all experiments described in this paper.

CH_4	760 ppb
N_2O	270 ppb
CFCs	0
O_3	Local modern
Solar Constant	$1365 W/m^2$
Eccentricity	0.016724
Obliquity	$23.446°$
Perihelion	$102.04°$
Dynamic vegetation	Off
Deep-water overflow parametrization	Off

Table 2. Mean annual surface air temperatures (MASAT) and Equilibrium Climate Sensitivity (ECS)

Model	MASAT (°C)	ΔT with $E^{280}{}_P$ (°C)	ΔT with $E^{400}{}_P$ (°C)	ECS ($°K/2\times CO_2$)
$Eoi^{400}{}_P$	16.8	3.8	1.8	7.4
$Eoi^{450}{}_P$	17.3	4.3	2.3	6.3
$E^{280}{}_P$	13.0	—	—	—
$E^{400}{}_P$	15.0	—	—	—

Table 3. Mean seasonal surface air temperatures and anomalies.

	Control		Pliocene		Anom w.r.t $E^{280}{}_P$		Anom w.r.t $E^{400}{}_P$	
Season	$E^{280}{}_P$	$E^{400}{}_P$	$Eoi^{400}{}_P$	$Eoi^{450}{}_P$	$\Delta Eoi^{400}{}_P$	$\Delta Eoi^{450}{}_P$	$\Delta Eoi^{400}{}_P$	$\Delta Eoi^{450}{}_P$
DJF	11.3	13.3	14.4	15.0	3.1	3.7	1.1	1.7
MAM	12.9	14.9	16.7	17.3	3.8	4.4	1.8	2.4
JJA	14.9	16.8	19.2	19.7	4.3	4.8	2.4	2.9
SON	13.0	15.0	16.7	17.2	3.7	4.2	1.7	2.2

Clim. Past Discuss., doi:10.5194/cp-2017-21, 2017
Manuscript under review for journal Clim. Past
Discussion started: 24 February 2017

Climate of the Past Discussions
Open Access
EGU

Table 4. Models details and diagnostics.

Model	Description	CO_2 (ppmv)	Vertical mixing	Simulation Length (yr)	Energy Balance TOA (Wm^{-2})	AMOC strength (Sv)
E^{280}	PI Control	280	$0.16\,cm^2s^{-1}$, constant	4,650[a]	0.02	20
E^{400}	Modern Control	400	$0.16\,cm^2s^{-1}$, constant	1,750	0.08	21.9
Eoi^{400}	Pliocene	400	$0.16\,cm^2s^{-1}$, constant	1,350	0.06	21.2
Eoi^{450}	Pliocene	450	$0.16\,cm^2s^{-1}$, constant	1,150	0.14	21.4
$E^{280}{}_P$	PI Control	280	POP1 type	5,170[ab]	0.11	21.5
$E^{400}{}_P$	Modern Control	400	POP1 type	1,970[c]	0.17	24.2
$Eoi^{400}{}_P$	Pliocene	400	POP1 type	2,700[d]	0.1	23.4
$Eoi^{450}{}_P$	Pliocene	450	POP1 type	2,650[e]	0.1	23.7

[a]Includes 3,500 years from existing control simulation
[b]Includes 630 years from model E^{280}
[c]Includes 360 years from model E^{400}
[d]Includes 1,120 years from model Eoi^{400}
[e]Includes 1,050 years from model Eoi^{450}